DETERMINATION OF ROOT LENGTH OF EVAPOTRANSPIRATION COVER USING ELECTRICAL RESISTIVITY IMAGING TECHNIQUE

by

FOUZIA HOSSAIN OYSHI

Presented to the Faculty of the Graduate School of

The University of Texas at Arlington in Partial Fulfillment

of the Requirements

for the Degree of

MASTER OF SCIENCE IN CIVIL ENGINEERING

THE UNIVERSITY OF TEXAS AT ARLINGTON

May 2018

Acknowledgements

First, I would like to express my deepest gratitude to my supervisor, Dr. Sahadat Hossain, for sharing his valuable time and giving me guidance, encouragement, help, and unconditional support throughout my master's studies. Without his constant guidance and support, this thesis would not have been completed.

I would like to express my gratitude to the City of Irving Landfill, specially Brenda A. Haney (Director, City of Irving Solid Waste Services) and Bill Sangster (Landfill Manager, City of Irving Solid Waste Services).

I would also like to give special thanks to Dr. Xinbao Yu and Dr. Melanie L Sattler, for their time and participation as my committee members, and for their valuable suggestions and advice.

Special thanks are extended to Jobair, Asif, Lucas, Cory, Sachini, Dola, Ziaul, Basit, and Naima for their active cooperation and assistance in all stages of work. I wish to acknowledge the cooperation, sacrifice, and unconditional support that I received from my husband, Ashraful Arefeen, throughout my graduate studies. I would like to thank my sister, Meher Niger Etho, and brother, Nazmus Sayadat, for their support. I would like to thank my in laws for their unconditional support. Finally, and most of all, I would like to thank my parents for all their love, encouragement, and great support.

April 13, 2018

Abstract

DETERMINATION OF ROOT LENGTH OF EVAPOTRANSPIRATION COVER USING ELECTRICAL RESISTIVITY IMAGING TECHNIQUE

Fouzia Hossain Oyshi, MS

The University of Texas at Arlington, 2018

Supervising Professor: MD Sahadat Hossain

Evapotranspiration (ET) covers are receiving an increasing amount of attention for use at waste disposal sites. Instead of using barrier layers like conventional covers, percolation in ET cover system is minimized by water balance components which store the water prior to its transpiration through vegetation or evaporation from the soil surface. Vegetation for an ET cover must be suitable for its particular locality and have well-developed root systems, since they promote transpiration and contribute to the long-term performance of the cover. They pull water out of the cover soil and release it into the environment, thereby decreasing the percolation of water through the cover and increasing the amount of transpiration that takes place through the roots. Unusually deep rooted vegetation, however, can penetrate the waste area, resulting in the transport of constituents to the above-ground biomass. Thus, determination of root length is very important for the ET cover design. But, the study of plant roots conventionally includes destructive and time-consuming methods. Destructive methods do not allow root measurements to be repeated at the same location, but only a handful of studies focus on non-destructive root studies, which are restricted by the soil and root type. Among the non-destructive techniques, electrical resistivity imaging is one of the most popular methods. Resistivity Imaging (RI) is a non-destructive method used to investigate the subsurface condition, during which an electrical current is applied to the soil through conductors known

as electrodes, so that the differences in the electrical potential at each specified location can be measured. It is considered that, roots affect in creating difference in electrical potential. The difference in potential creates the feasibility for studying root properties in the soil by electrical resistivity imaging. The objective of the current study was to determine the root length of vegetation in an ET cover soil, using the RI method. Two ET covers located in two slopes at the City of Irving Landfill in Irving, Texas were investigated, using the RI method, to estimate root length. The determination of the root length was also studied based on the minirhizotron technique to measure the actual root length in the site. The estimated root lengths were compared with the actual root lengths. The estimated root lengths were 1.9 feet and 1.2 feet, whereas corresponding actual root lengths were 1.75 feet and 1 foot, respectively. An analytical model was developed to determine the root length based on its relationship with resistivity and precipitation. Predicted root lengths from the developed model were within a band of 15% error margin of the actual root lengths, indicating good agreement between the actual and predicted values.

Table of Contents

List of Illustrations

List of Tables

Chapter 1

INTRODUCTION

1.1 Background

The US government spends billions of dollars every year to close dump sites and to monitor post-closure to minimize the environmental degradation from landfills. The final cover system is considered one of the most significant components of landfills for waste containment (Albright et al., 2004; Bonaparte et al., 2002; Alam, 2017), as it is responsible for significant harm to the environment if it is not designed and constructed properly. Therefore, the final cover system is the key element of a landfill.

There are two types of cover systems: conventional covers and evapotranspiration (ET) covers. Conventional landfill covers have been widely implemented throughout the United States in the past, but many state regulatory agencies and landfill operators are currently attracted to the evapotranspiration (ET) cover because of its advantages over the conventional types. An ET cover is effective in terms of performance, cost effectiveness, and longevity. It absorbs, holds, and releases precipitation in order to minimize percolation into the waste mass. (Rock, 2010). The major two components of an ET cover are soil and plants, and monitoring the length of the plant root that extends into the cover soil is one of the most crucial and important tasks that is performed to evaluate its performance. The rate of transpiration or water removal from the ET cover relies, to a large extent, on the plant root characteristics. The evapotranspiration depth depends on the rooting depth and parameters describing root length density functions of vegetation (Khire, 1997). Thus, it is very important to maintain a healthy plant root system to effectively and reliably remove infiltrated water (Hauser, 2009), and monitoring the root growth is important for evaluating the ET cover's performance.

Root growth and measurements have been studied by researchers for the last few decades to gain knowledge pertaining to root development, position, distribution, and penetration depth. The information on root growth is very significant (Weaver et al., 1922). Several studies have also been conducted on the determination of root length of vegetation. Traditionally, trench, photographs and drawing methods, pin boards, monoliths, augurs, and core methods have been used for root study. Methods usually employed to study tree roots are destructive, labor intensive, and time consuming; only a handful of small scale studies, strongly limited by soil conditions and root size, have utilized nondestructive techniques (Amato et al., 2008). Soil electrical resistivity, measured by geoelectrical methods, has the potential to detect below-ground plant structures (Amato et al., 2008), and electrical resistivity tomography is one of several non-destructive methodologies that is being tested (Paglis, 2013). Multichannel electrical resistivity is a popular geophysical exploration technique. The physical principle of the technique is simple, and the data acquisition is efficient. Traditional resistivity measurements are carried out on the earth's surface with a specified array to obtain apparent resistivity sounding curves, apparent resistivity profiling, and apparent resistivity pseudo sections. The resistivity profile qualitatively reflects vertical or horizontal variations in subsurface resistivity (Khan, 2011). The roots in the soil create a disturbed soil zone, which may cause some variations in the resistivity imaging; the variations can be used to interpret root length inside the soil transect.

1.2 Problem Statement

In spite of being a viable potential landfill closure technique, the ET cover still has some drawbacks due to the lack of effective non-destructive testing methods for quantifying the plant roots to evaluate its overall performance. At present, different destructive methods are utilized, to a large extent, to investigate the unknown root depth. The typical methods

available for root quantification are: trench; photographs and drawing methods; pin boards; monoliths; augurs; and core, all of which are highly invasive and can destroy the integrity of the ET cover. A large portion of soil needs to be excavated for root quantification, resulting in a high possibility that the ET cover will malfunction. Moreover, these methods are tedious, time consuming, and render a single-time measurement, meaning that every time the roots need to be monitored, a large portion of the soil will have to be excavated.

In this study, 2D electrical resistivity imaging was utilized to investigate unknown root length at two final covers located in the City of Irving Landfill in Irving, Texas. The root lengths determined from 2D resistivity imaging were compared to the actual root length observed by the minirhizotron technique.

1.3 Objectives

The overall objective of this study was to determine the unknown root length of an ET cover, using the ERI technique. To accomplish the objective, the following tasks were executed:

- Performance of electrical resistivity imaging in the site at regular intervals;
- Estimation of root length, using ERI data;
- Quantification of root length of ET cover, using the minirhizotron technique;
- Comparison of root length estimated using ERI data and measured using the minirhizotron technique;
- Development of a correlation between plant root length and ET cover soil resistivity.

1.4 Organization

A brief summary of the chapters included in this thesis is presented below.

Chapter 1 presents the significance of the subject matter, problem statement, and objectives.

Chapter 2 presents a literature review on the evapotranspiration (ET) cover system. This chapter also includes methodologies for root measurements and the concept of electrical resistivity imaging, as well as a brief review of available array methods.

Chapter 3 describes the characteristics of ET cover soil and details of the field investigation program for determining root length, using 2D resistivity imaging and the minirhizotron technique.

Chapter 4 presents an analysis of electrical resistivity imaging test results for unknown root lengths. An analytical model is also presented in this chapter for determination of root length based on the relationship between the electrical resistivity and the amount of precipitation. The test results for the technique based on minirhizotron is also compared with the RI test results.

Chapter 5 includes a summary of the study and provides recommendation for future research.

Chapter 2

LITERATURE REVIEW

2.1 Introduction

A landfill final cover is a multi-layered system, composed of different materials; it is the most important component of a landfill. Environmental degradation is predominantly linked with failure of the final cover system. Three primary goals can be achieved by constructing a final cover over a landfill; namely, waste isolation, infiltration minimization, and control of fugitive gas emissions (Hauser et al., 2004). There are two basic types of final cover systems: conventional or prescriptive final covers, and alternative final covers.

2.2 Landfill Cover Systems

USEPA 2011 defines a landfill cover as a critical component of landfill operations. Its function is significant in reducing environmental damage posed by the landfill, making it very important that each application of cover is appropriate for controlling possible threats. Cover technology can be innovative or conventional. Whatever the technology, it has to coordinate effectively with other parts of the landfill system, including gas collection, groundwater protection and leachate management systems (Koerner, 1997). There are several types of landfill covers, and the choice of which one to use depends on the type of use at different times of active life of the landfill. The general types of covers are daily cover, intermediate cover, and final cover. The working face of the landfill is covered by a daily cover after working hours to prevent birds and rodents from invading the waste and litter and to keep odor from spreading. The inactive parts of the landfill, which may receive waste in future, are covered by intermediate covers. The most significant cover for landfill is the final cover. It belongs to the process of landfill remediation. After the landfill reaches its design capacity for final waste, the final cover is put in place (McBean et al., 1995; Dunn,

1995). For this study, the cover system referred to henceforth will be the final cover system of the landfill.

2.2.1 Requirements for Landfill Covers

The following are the goals of final covers (Hauser, 2009):

- To minimize the amount of water that infiltrates the landfilled waste, resulting in contaminated water percolation into the groundwater;
- To quarantine wastes to prevent them from being dispersed into the environment;
- To control the emission of landfill gases.

2.2.2 Conventional vs Alternative Cover System

The Resource Conservation and Recovery Act (RCRA) established regulations for the design of conventional final cover systems in the United States; modified versions are used by individual states. A cover less permeable than the landfill bottom liner is required by regulation to avoid the “bathtub effect.” A conventional cover is usually underlain by a geomembrane layer, which is placed over a compacted clay liner or low permeability soil (with the order of 10^-5 to 10^-7 cm/sec). In locations where clay soil with low permeability is not available, a geosynthetic clay liner is used. The cover is installed above the layers. (Goldenberg, 2017). The only exceptions are found in some older landfills that were constructed without a geomembrane layer.

The alternative, or evapotranspiration (ET), landfill cover is a nature-friendly system, where the cover works with nature’s components to prevent water from entering the landfilled waste. The most important characteristics of the ET cover are it is not comprised of any barrier layer, and it functions well for a long period of time. The natural processes are: (1) The cover soil acts as a water reservoir, and (2) evaporation and

evapotranspiration move the reserved water into the atmosphere. Figure 2.1 shows schematics of conventional and alternative covers.

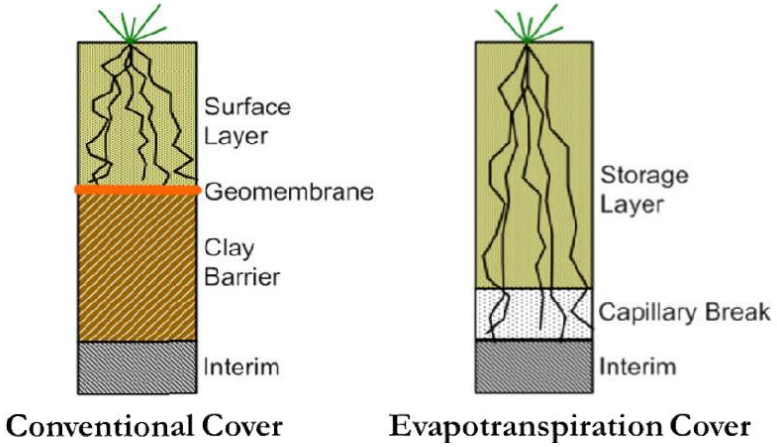

Figure 2.1 Conventional and alternative landfill covers (Benson and Bareither, 2012)

2.2.3 Cost Comparison

Hauser et al., 1999 reported that the construction cost for a conventional landfill varies between $319,000 and $571,000 per acre of surface cover, and that the cost of a landfill with an ET cover is approximately half of that. In 2001, Hauser et al. reported that the construction cost of an ET cover can vary between 35% and 72% of the construction cost of a conventional cover. Artificial processing is needed by an ET cover, which makes the maintenance cost lower than that of a conventional cover, and the repairs are also less expensive.

2.2.4 Advantages and Disadvantages

An ET cover is an effective, natural, and self-subsistent landfill cover that generally meets the requirements of cover for a site and costs about half that of a conventional cover. Different waste containment facilities, such as municipal, industrial, or hazardous landfills, are suitable for ET covers, depending on the site condition. Different types of functions can be performed by an ET. If there is a site requirement of no or minimum percolation, the ET

cover can be designed according to that requirement. On the other hand, because of flexibility of design and construction, it can also allow infiltration of water for bioreactor landfill purposes. Table 2-1 summarizes the advantages and disadvantages of the ET cover.

Table 2-1 Advantages and disadvantages of ET landfill covers (Hossain, 2017)

Advantages	**Disadvantages**
Natural System	Site specific design is required
More possibility of long term success	Requires adequate soil availability nearby
Long life	Restriction for reusable use
More protective to human and environment	
Easy maintenance	
Low construction cost	
Easily adaptable to bioreactor systems	

Site specific parameters are applied in the design and construction of an ET cover. The parameters include climatic conditions, available soils and their water storage capacities, the required soil thickness, and the available plant species' ability to uptake water. The design should be carefully evaluated to ensure that is able to control intake of water. An ET cover with proper design is potentially more advantageous since barrier and drainage layers are not needed. Less energy is required for mixing, engineering, placing, and compacting soils. There are some disadvantages to ET cover systems too. They might not be appropriate at facilities that have insufficient evapotranspiration to remove the precipitation from the soil column, or where the geology is unfavorable. There is also the possibility that an agency may not accept them, and costs may increase with test pads. The USEPA initiated the Alternate Cover Assessment Program (ACAP) in 1998 for evaluating the field performance of traditional and alternate landfill covers (Albright et al., 2010). ET covers were installed at 12 sites, where their performance was highly variable, with percolation rates ranging from 0 to 207 mm/yr. A strong relationship was found between performance and climate. The lowest percolation rates occurred in arid or semi-

arid climates, and the highest rates were measured in sub-humid and humid climates. If required soils were available nearby, then the cost of the ET cover remained low, but when the thickness of the soil was high, almost 3 meters in some cases, the cost of transportation of a large quantity of soil sometimes exceeded the cost to construct a traditional composite cover system. There are potential limitations as to where ET covers can provide low permeability in dry climates. If they are designed and constructed with appropriate soils, thicknesses, and sustainable vegetation, they are capable of meeting regulatory requirements at exceptionally lower costs than traditional cover systems.

2.3 Evapotranspiration Cover System

ET cover systems rely on the soil layer to store precipitation until natural evaporation or transpiration by vegetation occurs. They differ from conventional cover designs in that they rely on achieving appropriate water storage capacity in the soil instead operating as an as-built, engineered, low hydraulic conductivity. Designs of ET cover systems are based on using hydrological processes like water balance components at a site. The processes include water storage capacity of the soil, precipitation, surface runoff, evapotranspiration, and infiltration. The potential for percolation through the cover system reduces with greater storage capacity and evapotranspirative properties.

ET cover system designs tend to emphasize the following (Dwyer, 2003; Hakonson, 1997; Hauser, Weand; and Gill, 2001b):

- Soils with higher storage capacity like silts and clayey silts,
- Proper vegetation for long-term stability and evapotranspiration,
- Soils available locally for efficient construction and cost savings.

Local soils provide an opportunity to utilize natural analogue data to investigate future performance. In addition to being called ET covers, literature refers to these covers as water balance covers, alternative earthen final covers, vegetative landfill covers, soil-

plant covers, and store-and-release covers. A monolithic soil barrier is used to build ET cover systems. (Monolithic covers are also referred to as monofill covers.) Monolithic covers use a single, fine-grained soil layer to retain water and support vegetation (Albright et al., 2010 and Hauser, 2009). Figure 2.2 (a) shows a schematic of a monolithic ET cover. A capillary break can be added to modify a monolithic cover, but it requires placement of a coarser grained material, mostly sand or gravel, beneath the monolithic fine-grained soil, as shown in Figure 2.2 (b). Differences in the unsaturated hydraulic properties (i.e. soil matric potential) between the two layers minimize percolation into the coarser grained (lower) layer under unsaturated conditions (Stormont, 1997). Even after adding a coarser layer, the finer-grained layer has the same function as the monolithic soil layer. It stores water until it is removed from the soil by evaporation or transpiration mechanisms; however, the disruption in pore sizes between the coarser-grained and finer-grained layers gives rise to a capillary break at the interface of the two layers. Absorption of water into unsaturated pore space in the finer grained soil results in the capillary break, allowing the finer-grained layer to retain more water than a monolithic cover system of equal thickness. Water is held by capillary forces in the finer-grained layer prior to the saturation of the soil interfaces. If the finer-grained layer reaches saturation, water moves relatively quickly into and through the coarser-grained layer and eventually to the waste below (Albright et al. 2010; Hauser 2009; ITRC 2003).

Not only are ET covers are less costly to construct, but they also potentially provide equal or superior performance compared to conventional cover systems, especially in arid and semi-arid environments, where they may be less prone to deterioration from desiccation, cracking, and freezing/thawing cycles. They may also be able to minimize side slope instability, because they do not contain geomembrane layers, which can cause slippage (Albright and Benson, 2005; Benson et al., 2002; Dwyer et al., 1999).

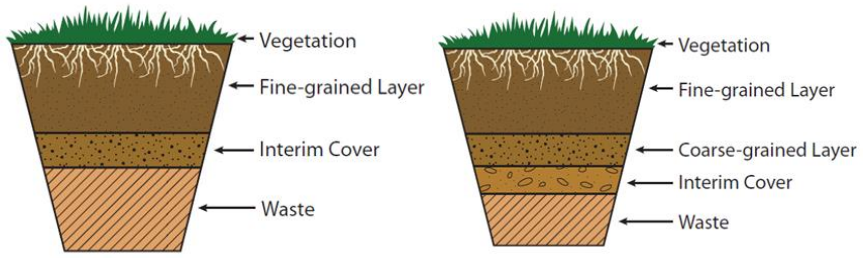

(a) (b)

Figure 2.2 Conceptual design of ET cover: (a) Monolithic ET cover, (b) Capillary barrier ET cover

2.3.1 Water Balance Equation

The water balance equation which governs the inflow, outflow, and storage changes in these types of covers can be expressed as follows:

$$Pr = P - R - ET - \Delta SWS$$

Where;

P is the precipitation, R is the runoff, Pr is the percolation through the bottom of the cover system, ET is evapotranspiration, and ΔSWS is the change in soil water storage over an arbitrary period of time. Figure 2.3 shows a schematic of the water balance equation.

The total quantity, form, and distribution of precipitation have a large effect on the water storage capacity of the cover system (Rock et al. 2012). In particular, if the cover system is required to accommodate a spring snowmelt, resulting in a large quantity of water being at the cover; and when there is relatively low PET (potential ET), with persistent light precipitation. The cover system should have enough storage capacity in dormant periods of vegetation (low PET).

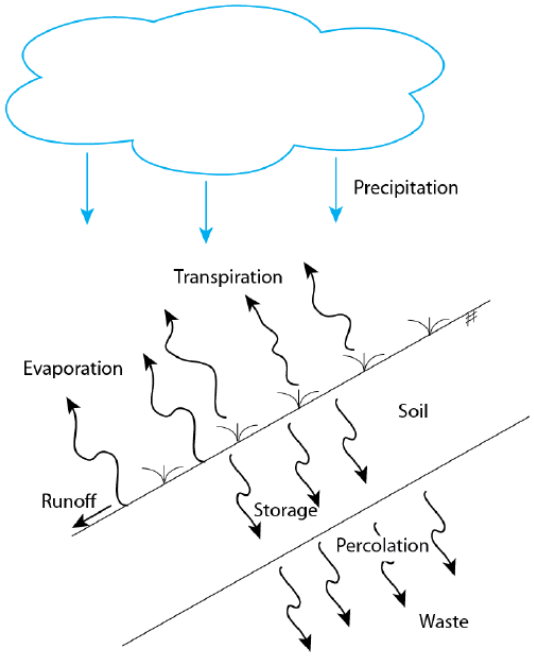

Figure 2.3 Schematic representing the cover system water balance for a landfill

Principal factors affecting surface runoff can generally be grouped into two major types: (1) climatic factors (rainfall duration and intensity, season, and the meteorological and frozen soil conditions prior to the storm)and (2) watershed factors (land slope, shape, soil, and land use). Rainfall intensity and duration affect the total quantity of runoff from a particular precipitation event. In the initial stages of precipitation, the infiltration rate into a cover system normally reduces. Consequently, because of a higher intensity precipitation, there might be little or no runoff. On the other hand, a substantial amount of runoff can be produced by a lesser intense precipitation of longer duration. The effect of a slope on runoff is critical. Typically, landfills are built on sites with a relatively steep side slope and a relatively flat top deck. The pools of water that form and the reduction of runoff are results of a depression in the soil's surface. Significant influence of vegetation growing on cover soil remains on runoff. In comparison to bare soil, greater percolation (lowest runoff) occurs in grasslands. Vegetation root systems perforate the soil, making the soil unconsolidated and

porous, and increase the infiltration and decrease the runoff rate. Vegetation reduces the velocity of the surface flow and provides more time for infiltration to occur by providing obstructions to runoff and surface roughness.

Transpiration is the process by which water, in liquid or solid state, is transformed into water vapor and enters the atmosphere. It occurs through the small openings in the vegetation tissues (e.g., leaves) and only occurs during hours of photosynthesis (typically only during daylight hours). The combination of evaporation and transpiration is known as evapotranspiration (ET). The maximum ET is referred to as potential ET (PET). ET is affected by several factors, as follows:

- Temperature – the rate of ET decreases with decrease of temperature;
- Humidity – the rate of ET decreases with increase of humidity;
- Wind speed – the rate of ET increases with increased wind speed;
- Water availability – ET will not occur if the cover system is dry;
- Soil type – the type of soil determines ease with which water is removed by ET; and
- Plant type – as discussed previously, some plants are able to remove more water from the soil than others, and the rate of transpiration differs for various plant species.

A critical design feature of ET cover systems is the ability of the cover soil to provide sufficient water storage capacity to control moisture and water percolation into the underlying waste. The storage capacity of the ET cover system is usually determined by the unsaturated and saturated hydraulic properties of the cover soil, soil type, soil thickness, and other factors which might result in an increase or decrease in the ability of soil to store water. The thickness required of the storage layer depends on the required storage capacity and is based upon the other water balance factors. The storage layer(s)

may be required to accommodate time periods when ET rates are low, when plants are dormant, or in extreme weather conditions (e.g., extreme precipitation events or snowmelts). Naturally, a thicker layer in the cover system results in greater storage capacity.

2.3.2 Plants and Plant Roots

The potential of an ET cover is optimal when the growth of its vegetation is limited only by the water content of the soil. Plants absorb water and nutrients quickly when growing conditions are good, and healthy plants minimize percolation from the bottom of the cover by drying the soil. Plant growth is limited to several factors, including soil properties, selection of the wrong species, temperature of soil and air, plant diseases, humidity, and insect attacks. The vegetation of an ET cover enhances transpiration and minimizes erosion since the vegetation stabilizes the surface of the cover. Grasses (wheatgrass and clover), shrubs (rabbit brush and sagebrush), and trees (willow and hybrid poplar) have been used on ET covers. Grass covers are preferred for some sites due to the need for prime erosion control and a substantial fibrous root system, but woody plants are preferred for others. Both warm and cold season species are usually planted and include native plants because of their tolerance for territorial weather conditions. Native plants consume available resources effectively and survive for a long period of time, even when they are grown in unfavorable conditions and are subjected to extensive droughts, insect attacks, and/or periodic fires and diseases. The mixture of warm and cold season species enables water uptake and promotes transpiration over the total growing period. Furthermore, imported plants are more like to disturb the natural ecosystem than native plants. They tend to dominate native species and can result in a monoculture forming which is not tolerant of unexpected incidents like sudden insect attacks and diseases.

It is not difficult to control the soil density during the construction of an ET landfill cover. The growth of roots slows when the soil bulk density is greater than 1.5 Mg/m3. When it is greater than 1.7 Mg/m3, it prevents roots from growing. Particle size distribution also plays role in controlling root growth. According to Jones (1983), root growth is reduced when the soil bulk density is greater than 1.5 Mg/m3 and in soils containing less than 70% sand and bulk density greater than 1.7 Mg/m3, 0.2. Robust root growth can be found in soils with a bulk density of 1.1-1.5 Mg/m3. ET covers of landfills are extremely dependent on the performance of plant roots. They are the controlling factor for water removal from the soil, and many complex functions are performed by them, including the following.

- Roots equip plants with an anchorage system.
- Fleshy roots act as storage for nutrients.
- Roots supp.ly plants with water and nutrients from the soil layers.
- Some plants are capable of developing random shoots when the main root gets damaged, allowing the benefits they provide to continue.

Plant roots remove water, nutrients, and oxygen from the soil. The shortest roots absorb water and nutrients present in the soil and oxygen from the soil atmosphere. When the soil gets dry, the plants get stressed, and the mass of shoots aboveground is reduced, causing the roots to dry. A favorable soil environment is important so that the plants can replace the dead roots quickly when favorable conditions return. It is very important that plants rapidly produce new roots in the wet soil after rainfall events, and native plants are more likely than imported plants to be able to do that. Low soil strength, sufficient fertility, and oxygen provide a favorable environment for root growth. Low strength of soil leads to low bulk density, which is very important for robust growth of vegetation and the success of an ET cover. The drying of each soil layer depends on the distribution and density of living plant roots. A general root distribution pattern for a soil with good tilth is shown in

Figure 2.4 below. When all layers are wetted in the growing season, roots develop as portrayed by condition 1. The majority of roots are in the upp.er 15-30 cm, near the surface, and when soils are wet, plants usually extract water and nutrients from uppermost layer. Thus, in a natural rooting pattern, the uppermost layer dries first, and the rooting pattern enters condition 2 when the upper layers Are dry. At the end of the growing season or after severe drought, the rooting assumes a pattern of condition 3, deep inside the soil profile. While parts of the root system die due to drying of the soil or other stresses, roots grow rapidly in other layers. Soil temperature, amount of oxygen, an other factors limit root density and water use from a soil layer. The density of living and active roots changes more than once during the season of growth as the conditions change.

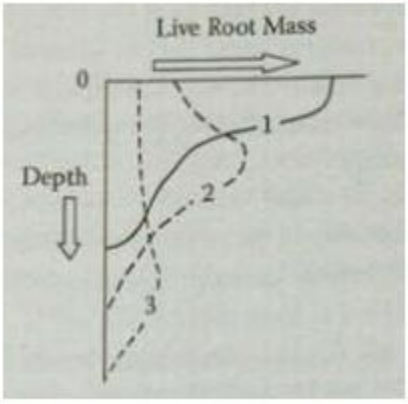

Figure 2.4 Possible distributions of living roots at different times during the growing season

When conditions are optimum, as in wet soil, plant roots grow faster; however, some factors may hinder root growth, such as:

- Undesirable soil pH
- Soil strength
- Physical factors
- Soil solution salinity

- Soil water content
- Soil oxygen
- Air-filled porosity in Soil
- Chemical toxicity
- Allelopathic toxicants.

2.3.3 Performance Criteria

The performance criteria of an ET cover includes:

- Control of infiltration into waste,
- Isolation of waste and prevention of its movement by wind or water,
- Control of landfill gas.

Design requirements for landfill covers are mandated by federal regulations that specify the water flow barrier, drainage layer, thickness and function of soil, and plant cover. An ET cover meets the performance criteria easily in most cases since it controls infiltration of water into the waste beneath the cover, separates the waste from the cover, and prevents its movement by wind or water. In a dry climate, where the cover soil is too thin to control the infiltration of water into the waste, increasing the thickness of the ET cover will usually solve the problem. It is also easy to install a conventional gas extraction system within an ET cover, where needed. For fresh waste, where there is a large amount of toxic gas or methane, it is a simple task to collect the gas by inserting a vertical gas well, which does not affect the performance of the ET cover.

The expense of constructing a landfill cover, in both time and money, is a major consideration. It is always important to measure the risks associated with the landfill and to consider what remediation will be necessary, how much time it will require, and what it will cost. For example, landfills located above tight shale or other low permeability materials are less prone to contaminating the ground water. On the other hand, in some old landfills,

the waste comes in contact with ground water, and the cover cannot protect the ground water from contamination.

2.4 Practices for Root Investigation

Researchers have studied root growth for many years. Determining the exact root development, position, distribution, and penetration depth are very important (Weaver et al. 1922) because every function of the roots is vitally important to the energy of the shoots. Weaver and Burner (1927) executed an extensive study on root size, but the amount of other literature available is limited because of the difficulty in studying underground structures. Having good perception about the distribution and structure of plant roots and root water uptake patterns has become increasingly important with the use of ET covers, where water dynamics is the main mechanism for sustainability. The structure of roots is one of the most important factors in soil-plant-water dynamics because it affects the pathway, water resistance, and movement of the solute. The extent of root the systems affects the volume of soil available, since soil is the source of water and mineral nutrients.

Knowledge of roots is of paramount importance to a vegetative landfill cover system, since the in-situ root depth and distribution of roots crucially affect the release process (transpiration) of water which is stored in the soil during a precipitation event (Barnswell and Dwyer, 2011, Benson et al., 2002; Khire et al., 2000; Malusis and Benson, 2006; and Stormont and Morris, 1998). Several methods have been devised for measuring the root systems. Each method requires a different technique, is performed with the use of different equipment, and has advantages and disadvantages. The advantages and disadvantages of the methods which are frequently used are listed in Table 2-2.

Table 2-2 Frequently-used methods for measuring and analyzing root systems (Alam, 2017)

Method	Information type	Destructive Method	Advantage	Disadvantage
Photographs or Drawings	Qualitative, 2D root morphology	✗	easy and rapid process, viewing exact root structure	tedious, blurry photographs, qualitative information only, root overlap, no statistical inference
Trench/Window	2D spatial root distribution	✓	Easy recording of root data, repeated same point measurement	Static, limited 2D area, destruction of roots during digging
Pinboards/Monoliths	Length, weight, diameter, distribution pattern	✓	provides natural arrangements of roots	labor intensive, skilled labor, loss of fine roots
Augure/Core	Length, weight, diameter, distribution pattern	✓	easy and straight forward method	requires large number of samples, labor intensive, time consuming, limited sampling depth
Rhizotron, Minirhizotron and Mesorhizotron	Dynamic 2D information, root growth and turnover	✗	repeated measurements at same point, accurate	expensive, labor intensive, time consuming

2.4.1 Typical Field Monitoring Methods of Measuring Root Growth

Several methods are used to measure root growth in the field. The horizontal and vertical glass plate method was used by McDougall (1916); the method of monoliths, soil cores, and profile walls was described by Schuurman and Goedewaagen (1965); and most recently, Smit et al., (2000) used the rhizotrons, minirhizotrons, or transparent walls/windows method. Some of the methods for root study are described in the following section.

One of the oldest methods for measuring roots is the trench Photographs and Drawings method, which was first used by Weaver et al. in 1922 and also incorporated the photographs and drawing method. In this method, a trench was dug along the side of the plant to a depth of five feet. The width of the trench was determined by the site condition and by the ease of digging it there. The major benefit of the method was that the entire root

system was visible after the excavation of the trench. However, the method has some drawbacks too, as the excavation of large trenches sometimes destroyed the roots, and photographs often became blurry. As a consequence, Weaver et al. (1922) proposed drawing life-sized images of the root system, emulating the exact measurements as closely as possible. Figure 2.5 shows a schematic drawing of the trench method.

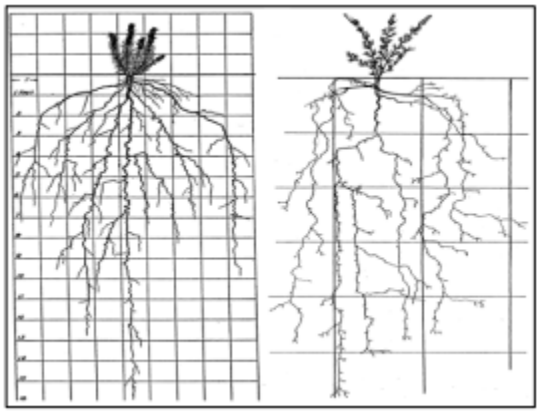

Figure 2.5 Root systems analyzed by excavation and drawing (Weaver, 1919; 1920)

The pinboard method provides a complete depiction of root structures, but its field installation is time consuming. A pit has to be excavated next to the plant, then the excavated wall is smoothed, and the pinboard is pressed against the wall. A steel cable is used so that the soil surrounding the pinboard is cut away, and the plant roots are still held by the pin when the pinboard is pulled away (Schuurman et al., 1971). Kono et al. (1987) and Kano-Nakata et al. (2011) quantitatively and qualitatively measured a root system, using a “root box-pinboard,” and reported that it was an easy and effective method for quantifying roots. It is not recommended for the ET cover, as the box limits the root growth (Kono et al., 1987).

Root development in the field is measured by an augur. The soil and root sample are extracted from the landscape, and the root sample is separated from the soil so that the roots can be quantified. Root growth is expressed as volume; diameter; weight; surface

area; root length density (RLD), which is root length per unit soil volume; and root mass density (RMD), which is root mass per unit soil volume (Barnett et al., 1983 and Bohm, 1979). Advantages of this method are that it needs only a portion of the root and the instruments required are not expensive. It follows a destructive procedure, however, and great potential for human error exists. Therefore, the augurs and cores method is not recommended for the ET cover system.

2.4.2 Advanced method : Rhizotron, Minirhizotron and Mesorhizotron

Rhizotrons are commonly used for root measurement. Rogers (1969) designed the first rhizotron, which was constructed in the East Malling district of Kent, England. “Rhizotron” is a combination of the Greek words “rhizos” for root and “tron” for instrument. It is an underground facility or structure through which plant roots can be viewed and measured through transparent surfaces which may remain in contact with the natural soil (Klepper et al., 1994). It is considered as one of the earliest non-destructive techniques for observing root growth in soil, and it allows repetitive measurements of root systems at a large field-scale. Rhizotrons have several advantages and limitations (Taylor et al., 1990). The most important advantage is that successive measurements are possible on the same individual root, allowing the rate of length increment of the root to be monitored (Taylor et al., 1990). Sensors and cameras are installed to evaluate soil conditions, and measurements are recorded with photography. Growth of the plant roots can be traced along the transparent wall, and the root density and speed of root growth can be determined (Glinski et al., 1993). However, this method is very expensive, both for the construction of the rhizotron and for operating it. (Taylor et al., 1990). At Auburn, Alabama in 1969, almost $40,000 was spent for a project to construct a rhizotron, and the cost of operating it for the first 13 years was from $50 -100,000. Updating the computer system and control system was included in the operating cost (Huck et al., 1982). Rhizotrons are

comparatively more expensive these days (Taylor et al., 1990). Huck and Taylor (1982) cited additional disadvantages of rhizotrons by pointing out that during its installation, the structure and the environment of the soil changes, and the surface from which to view the root may not be representative. Klepper et al. (1994) suggested changing the soil after the rhizotron research, as populations of worms, fungi, bacteria, and insects are very likely to grow there.

Bates (1937) proposed a minirhizotron as a viable alternative to rhizotrons. To observe roots, Bates used a mirror and a battery-operated lamp, and monitored roots intersecting in a glass tube in the ground. Later, the minirhizotron technique was improved upon by other researchers, to create the modern minirhizotron. The modern minirhizotron uses a color video camera, where images with better quality can be recorded in videos or photographs due to the application of modern technology (Smit et al., 2000; Dannoura et al., 2008; Taylor et al., 1990; and Patena et al., 2000). A schematic of the minirhizotron with a data acquisition system is shown in Figure 2.6.

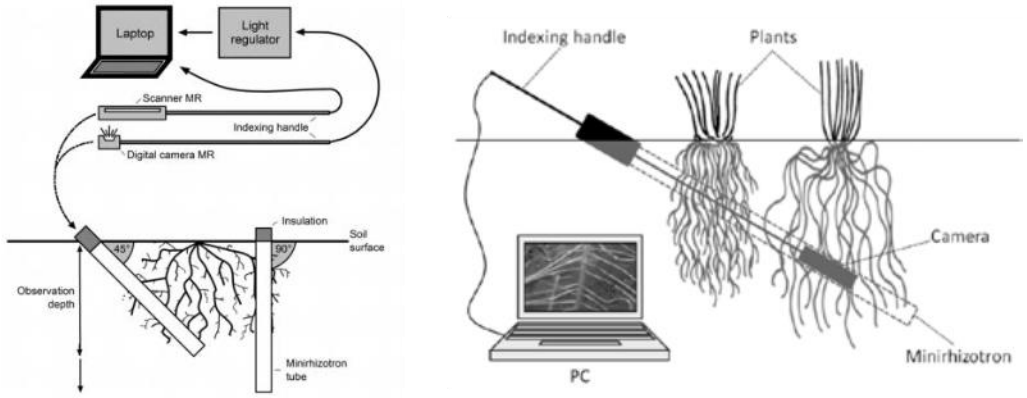

(a) (b)

Figure 2.6 Schematic diagram of minirhizotron tubes (a) in both angled and vertical positions (Modified from: Rewald and Ephrath, 2013), (b) Vamerali et al. (2012)

The minirhizotron is one of the best methods for studying roots. Same-point measurements can be found from it, and the only destructive part is during the 30 minutes

that are required to install it (Taylor et al., 1990). A substantial amount of time is required to collect the pictures from the tubes and analyze them (Ingram et al., 2001), but it is the best way to measure root growth and density and it preserves the maximum integrity of the ET cover.

2.4.3 Application of Electrical Resistivity Imaging (ERI) Technique

Electrical resistivity imaging (ERI) is a non-destructive and non-invasive geophysical method for measuring root biomass (Al Hagrey, 2007; Amato et al., 2008). Instant depth coverage and concentrated spatial data can be found from this subsurface geophysical investigation (Tabbagh et al., 2000) that can detect the resistive areas in the root zone (Al Hagrey et al., 2004). Extensive destructive sampling by Amato et al., 2008; Lazzari et al., 2008; Zenone et al., 2008; Panissod et al., 2001; Loperte et al., 2006; and Morelli et al., 2007 confirmed that variations of electrical resistivity (ρ) are related to plant roots.

The zone of evapotranspiration in contrasting vegetation types can be quantified by the application of the ERI technique. Jayawickreme et al. (2008) quantified the large seasonal differences in root-zone moisture dynamics for both forests and grasslands (Figure 2.7). It was demonstrated by them that ERI is a quick and easy method for quantifying the active zones of water uptake for different levels of soil water. Estimation of root water uptake in conventional methods is restricted to a one-dimensional approach, whereas both horizontal and vertical profiles are provided by ERI, linking the results more closely to field scale behavior. The consistence of electrical resistivity with hydraulic redistribution (HR), mostly hydraulic lift (HL) within the vadose root zone, was shown by Robinson et al. (2012). They concluded that the spatial information from the ERI method is much more complete and that it would have been difficult to obtain the necessary information through standard sampling.

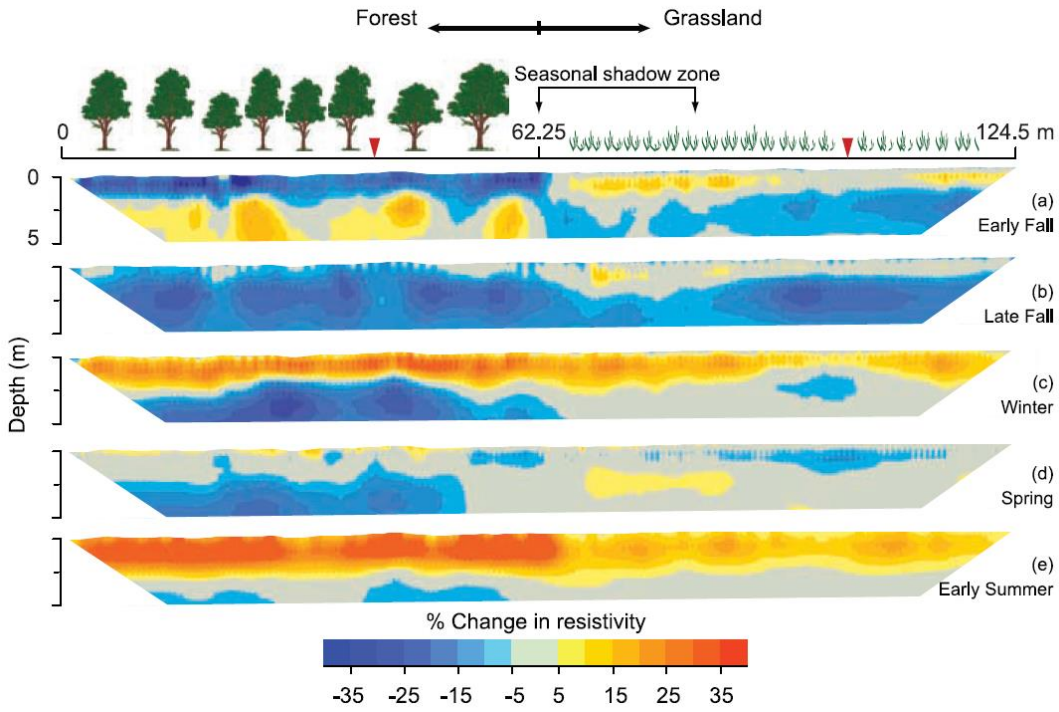

Figure 2.7 Subsurface imaging of root zone moisture (Jayawickreme et al., 2008)

2.5 Resistivity Imaging

One of the most popular and oldest geophysical techniques in electrical exploration is electrical resistivity. Electrical resistivity imaging is a non-invasive geophysical technique which provides a resistivity image of the subsurface that can be used for surface exploration, subsurface characterization, and monitoring. Utilization of this technique produces images of the subsurface with the aid of an automated data acquisition system and software that is user friendly. During 1920, the Schlumberger brothers conducted the first resistivity survey and it is still one of the primary methods used to measure electrical resistive properties of soil. Maganti, D., 2008 measured electrical resistivity by placing four electrodes in contact with the soil or rock. Electrical resistivity technology has advanced with increased sophistication of electrical hardware and software. Two methods are

available for subsurface imaging, using electrical resistivity. In the first method, electrical sounding is used to investigate depth, which provides information pertaining to a one-dimensional vertical profile with limited lateral variations. Telford et al., 1990, generated a lateral profile that uses electrical trenching, but it is limited to a constant depth. Multi-electrode systems can conduct both electrical sounding and electrical trenching at the same time. Today's advanced instruments can acquire the data as a set of sounding, consisting of a two-dimensional cross-section or resistivity profile of the subsurface. An accurate interpretation of the subsurface geologic setting can be made on the basis of the distribution of the resistivity profile (Maganti, D., 2008).

2.5.1 Theory of Resistivity

Resistivity distribution of soil volume is determined by an electrical resistivity survey. After supplying an electrical current to the soil, the resulting potential difference is measured. Information on the subsurface condition, as well as on the electrical properties, is provided by the measured potential difference pattern.(Kearey et. al., 2002). Electrical resistivity of the soil is considered as a proxy for the variation of soil properties (Banton et. al., 1997). For a simple body, the resistivity ρ (Ω m) is defined as

$$\rho = R(\frac{A}{L}) \quad \text{.....(2.1)}$$

Where R is the electrical resistance, L is the length of the cylinder (m) and A is the cross sectional area (m^2).

The electrical resistance of a cylindrical body is defined by the Ohm's law

$$R = \frac{V}{I} \quad \text{.....(2.2)}$$

Here, V is the potential difference measure in Volt and I is the current which is typically measured in Ampere. The conductivity (σ) is term reciprocal of resistivity.

Where,

$$\sigma = \frac{1}{\rho} \quad \text{.....(2.3)}$$

In a homogeneous and isotropic half space, electrical equipotentials are hemispherical, as shown in Figure 2.8 (Samouëlian et al., 2004). The current density J (A/m^2) is calculated for all the radial directions with,

$$J = \frac{I}{2\pi r^2} \quad \text{.....(2.4)}$$

Here, 2πr^2 is surface of a hemispherical sphere of radius r. The potential V can be expressed as,

$$V = \frac{\rho I}{2\pi r}$$

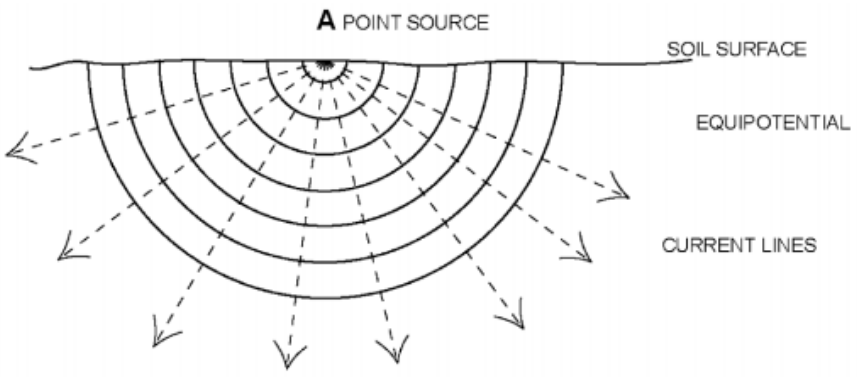

Figure 2.8 Distribution of current flow in a homogeneous soil (Samouëlian et al., 2004)

Four electrodes are necessary for measuring electrical resistivity. The two electrodes, A and B, are called current electrodes and inject current into the soil. The other two electrodes, M and N, are called potential electrodes. The potential differences due to current are measured by the potential electrodes. Figure 2.9 demonstrates the current and equipotential lines for one pair of current electrodes, A and B, on a homogeneous half-space.

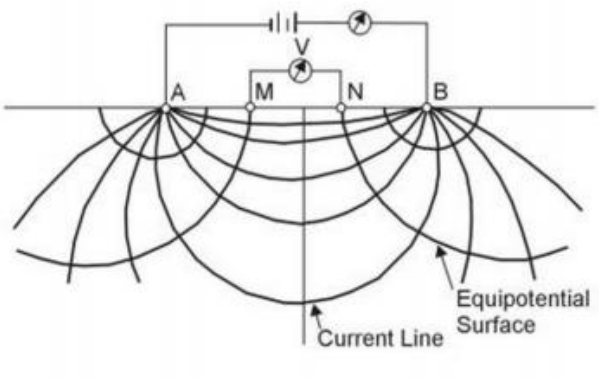

Figure 2.9 Equipotential and current lines for a pair of current electrodes, A and B (www.cflhd.gov).

The potential difference between the M and N is given by the equation,

$$\Delta V = \frac{\rho I}{2\pi}\left[\frac{1}{AM} - \frac{1}{BM} - \frac{1}{AN} + \frac{1}{BN}\right] \quad \text{.....(2.5)}$$

Where AM, BM, AN and BN are geometrical distance between the A and M electrode, B and M electrode, A and N electrode and B and N electrode respectively. The electrical resistivity is then calculated by the expression,

$$\rho = \frac{\Delta V}{I}\left[6\frac{2\pi}{\left(\frac{1}{AM} - \frac{1}{BM} - \frac{1}{AN} + \frac{1}{BN}\right)}\right] \quad \text{.....(2.6)}$$

Or,

$$\rho = \frac{K\Delta V}{I} \quad \text{.....(2.7)}$$

Here, K is the geometrical coefficient that depend on the arrangement of A, B, M, and N.

2.5.2 Variation of Electrical Resistivity as a Function of Soil Properties

Electrical resistivity is a function of different soil properties and depends on the nature of the solid constituents (particle size distribution and mineralogy); arrangement of the voids (porosity, pore size distribution, connectivity); degree of water saturation (water content); electrical resistivity of the fluid (solute concentration); and temperature. Air acts

as an insulator, which is infinitively resistive; the water solution resistivity is a function of the ionic concentration. The electrical resistivity of the solid grains is related to the electrical charge's density at the surface of the soil particles. The electrical resistivity of soil is dependent on the soil properties, but it varies in different ways and extent, according to Samouëlian et. al., 2004, who showed that the electrical resistivity for soil mapping can show a large range of values. The electrical resistivity in their research ranged from 1 Ω m for saline water to 105 Ω m for dry soil over crystalline rocks, as shown in Figure 2.10 (Samouëlian et al., 2004).

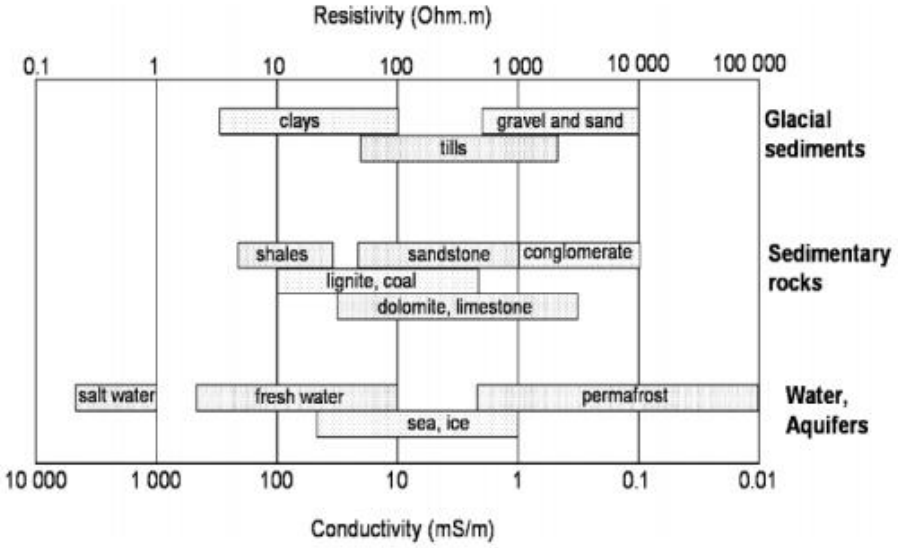

Figure 2.10 Typical ranges of electrical resistivity (Samouëlian et al., 2004).

2.5.3 Two-Dimensional Resistivity

A two-dimensional vertical picture of the sounding medium is provided by a two-dimensional multi-electrode array in two-dimensional resistivity. A fixed distance is maintained between the current and the potential electrodes in 2D resistivity imaging. At the soil surface, the electrodes are moved progressively along a line, and a measurement is taken at each step. A vertical profile of the resistivity values is provided by this set of measurements at the first inter-electrode spacing, and the second measurement is done

by increasing the inter-electrode spacing to n=2. The process with incrementing factor for n is repeated until reaching the maximum spacing. With larger n values, the depth becomes large. The 2D resistivity imaging technique is presented in Figure 2.11 (Samouëlian et al., 2004).

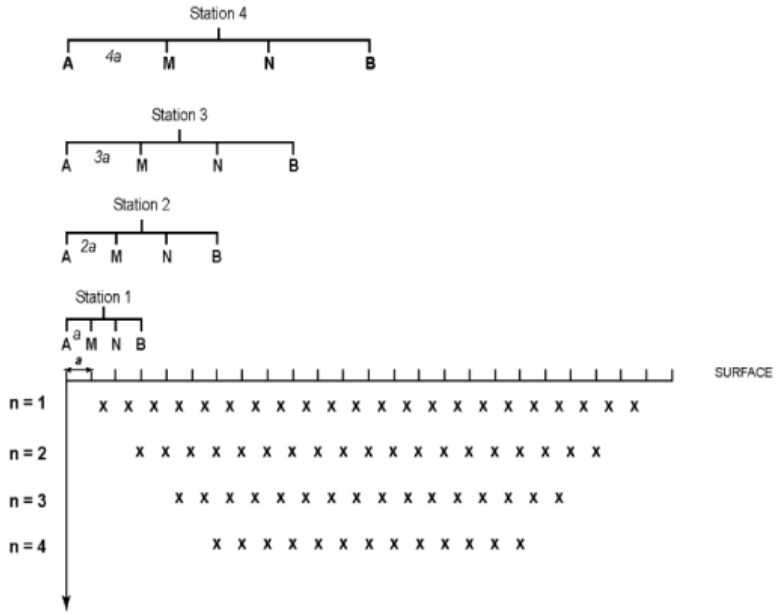

Figure 2.11 Establishment of a 2D resistivity imaging pseudosection (Samouëlian et al., 2004).

Current distribution is dependent on resistivity contrast of the medium. The investigation depth with the spacing is known as pseudo-depth. The data is organized in a 2D pseudosection plot that simultaneously displays both vertical and horizontal variations of resistivity. In the conventional graphic representation, each measured value is at the intersection of two 45° lines through the centers of the quadripole. The pseudo depth is given by each horizontal line which is associated to the n value (Samouëlian et al., 2004).

2.5.3.1 Electrode Array Configurations

Several array configurations are available, based on the position of the potential and current electrodes,. The most commonly used array configurations are Wenner, Wenner-Schlumberger, dipole- dipole, pole-pole, and pole-dipole. The configurations are presented in Figure 2.12. Geometrical factor k depends on the geometrical configuration.

		Electrodes array	K
2D	Wenner	A a M a N a B	2πa
	Wenner-Schlumberger	A na M a N na B	πn(n+1)a
	Dipole-Dipole	A a B na M a N	πn(n+1)(n+2)a
	Pole-Pole	B x A a M x N	2πa
	Pole-Dipole *Forward*	A na M a N	2πn(n+1)a
	Reversed	M na N a A	

Figure 2.12 Different array configurations for 2D resistivity Imaging (Samouëlian et al., 2004).

The array configuration has a significant influence on the resolution, sensitivity, and depth of investigation (Samouëlian et al., 2004). Table 2-3 summarizes the sensitivity of the array to vertical and horizontal heterogeneities, depth of investigation, horizontal data coverage, and signal strength. The median depth and total length of the different arrays are presented in Table 2-4.

Table 2-3 Characteristics of different 2D array configurations (Samouëlian et al., 2004)

	Wenner	Wenner-Schlumberger	Dipole-Dipole	Pole-Pole	Pole-Dipole
Sensitivity of the array horizontal structures	++++	++	+	++	++
Sensitivity of the array vertical structures	+	++	++++	++	+
Depth of investigation	+	++	+++	++++	+++
Horizontal Data Coverage	+	++	+++	++++	+++
Signal Strength	++++	+++	+	++++	++

The labels are classified form (+) to (++++), equivalent at poor sensitivity to high sensitivity for the different array configurations.

Table 2-4 Different median depth (Ze) and Length (L) covered by each array (Loke M. H., 1999)

Array type		z_g/a	z_g/L
Wenner alpha		0.519	0.173
Dipole-dipole	n = 1	0.416	0.139
	n = 2	0.697	0.174
	n = 3	0.962	0.192
	n = 4	1.220	0.203
	n = 5	1.476	0.211
	n = 6	1.730	0.216
Equatorial dipole-dipole			
	n = 1	0.451	0.319
	n = 2	0.809	0.362
	n = 3	1.180	0.373
	n = 4	1.556	0.377
Wenner - Schlumberger			
	n = 1	0.52	0.173
	n = 2	0.93	0.186
	n = 3	1.32	0.189
	n = 4	1.71	0.190
	n = 5	2.09	0.190
	n = 6	2.48	0.190
Pole-dipole	n = 1	0.52	
	n = 2	0.93	
	n = 3	1.32	
	n = 4	1.71	
	n = 5	2.09	
	n = 6	2.48	
Pole-Pole		0.867	

2.5.3.1.1 Wenner Method

The Wenner Method consists of four electrodes in a line with equal spacing. It is best suited for profiling because only one electrode is moved for measurements. A sensitivity plot of the array is presented in Figure 2.13 (Loke M. H., 1999).

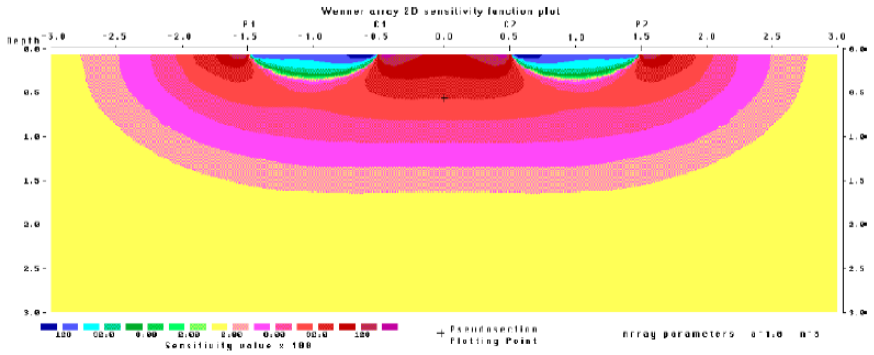

Figure 2.13 Sensitivity plot for Wenner array (Loke M. H., 1999)

The Wenner array is comparatively more sensitive to vertical changes in the subsurface resistivity and less sensitive to horizontal changes. With moderate depth of investigation, the Wenner array has the median depth of investigation of approximately 0.5 times the spacing of “a.” An inverse proportional relationship exists between the signal strength of the array and the geometric factor when the geometric factor is 2πa, which is relatively smaller. The array gets better signal strength, but the increasing electrode spacing results in poor horizontal coverage (Loke M. H., 1999).

2.5.3.1.2.Wenner Schlumberger Method

The Wenner Schlumberger Method is a modified form of the Schlumberger Method, and is a comparatively new method of electrical resistivity imaging. In this method, the electrodes can be spaced at constant spacing. Figure 2.14 presents the sensitivity pattern for the Wenner Schlumberger method.

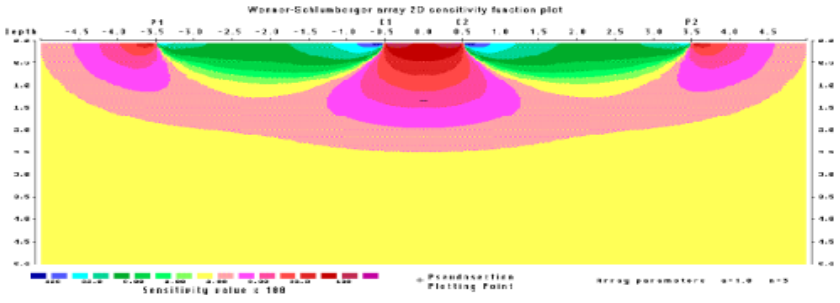

Figure 2.14 Sensitivity plot for Wenner Schlumberger array (Loke M. H., 1999)

The Wenner array has a very high signal strength compared to other methods. The Schlumberger method's signal strength lies between the Wenner array and the dipole-dipole array. The median depth of investigation (with the same distance between the outer current electrode) is about 10% higher for the Schlumberger array (Maganti, D., 2008), and the Wenner-Schlumberger array has slightly better horizontal coverage than the Wenner array (Loke M. H., 1999). The pseudosection data patterns for the Wenner and Wenner-Schlumberger arrays are presented in Figure 2.15.

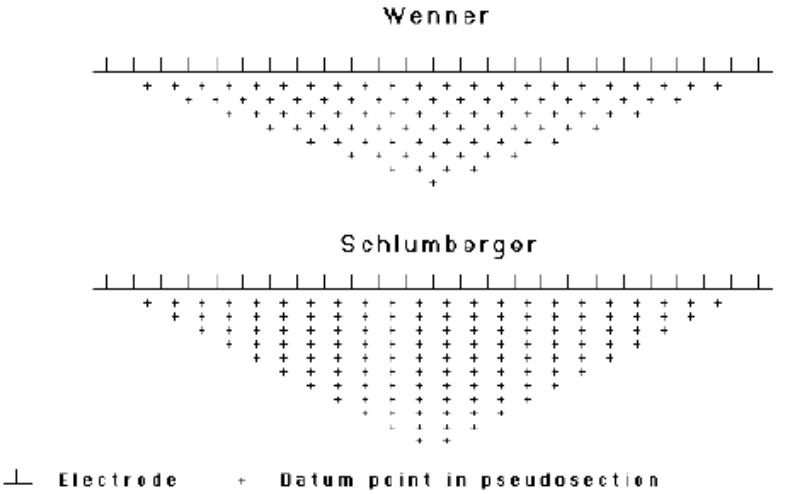

Figure 2.15 Pseudosection data pattern for the Wenner and Wenner Schlumberger arrays ((Loke M. H., 1999)

2.5.3.1.3 Dipole-Dipole Method

The most convenient array in the field is the dipole-dipole array. It can cover a larger space, with more spacing between the electrodes, depending on the desired depth of penetration, and provides the highest resolution. It is highly sensitive to vertical changes of resistivity, but comparatively not that sensitive to horizontal changes in resistivity, which indicates that the dipole-dipole array is good at mapping vertical structures, but not that good at mapping horizontal structures. The array is sensitive to changes of resistivity between the electrodes in each dipole pair, and the contour pattern of sensitivity is almost

vertical in the plot. However, variations of near-surface resistivity affect the dipole-dipole array data (Maganti, D., 2008). For each traverse (n), the electrode spacing and dipole separation are constant, then increase with each successive traverse. Higher electrode spacing gives greater penetration depth, but the resolution is poor. The sensitivity plot for the dipole-dipole array is presented in Figure 2.16.

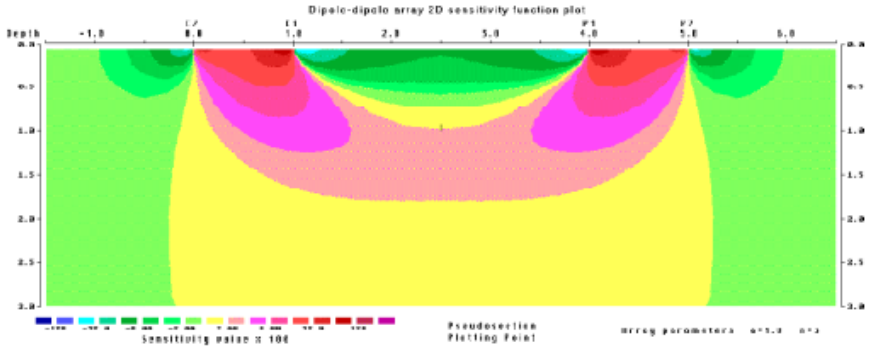

Figure 2.16 Sensitivity plot for dipole-dipole array (Loke M. H., 1999)

2.5.3.1.4 Pole-Pole Method

Pole-pole array is not as popular as the Wenner, dipole-dipole, or Schlumberger arrays. Although the ideal pole-pole array has only one current and one potential electrode, a second current and potential electrodes must be placed at a distance of more than 20 times the highest separation between first pair of current and potential electrodes. Potential electrodes are placed at large distance in the dipole dipole array which may be affected by huge telluric noise which might intensely degrade the quality of the measurement. Surveys using small electrode spacing typically use the pole- pole method, and archaeological surveys use it in a few applications (Loke M. H., 1999). It has the deepest depth, as well as widest horizontal coverage, with the poorest resolution. The sensitivity diagram for the pole-pole method is presented in Figure 2.17.

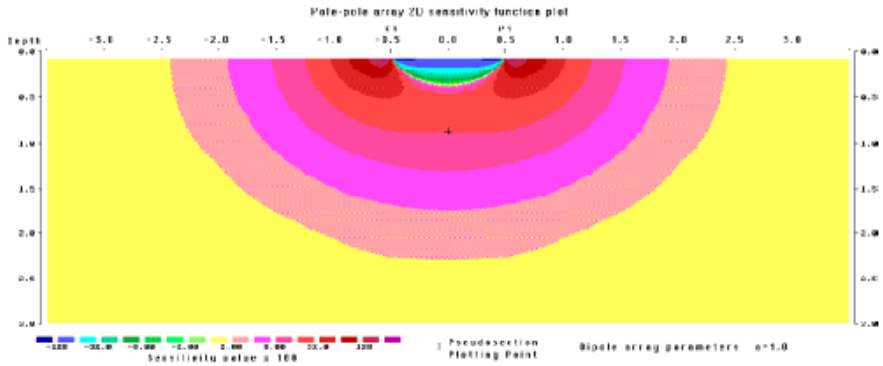

Figure 2.17 Sensitivity plot for pole-pole array (Loke M. H., 1999)

2.5.3.1.5 Pole-Dipole Method

The pole-dipole array is an asymmetrical array that can be effected by the asymmetry in apparent resistivity values after inversion. A reverse-order arrangement of electrodes can eliminate effect of the asymmetry. It is a combination of “forward” and “reverse” pole-pole arrays, and eliminates any bias in the model caused by the asymmetrical array. The signal strength of a pole-dipole array is significantly higher than a dipole-dipole array and is less sensitive than the pole-pole array to telluric noise. This array has relatively better horizontal coverage for determining resistivity; however, the signal strength is lower than the Wenner and Wenner-Schlumberger arrays, but higher than the dipole-dipole arrays.

2.5.4 Data Acquisition

After each measurement, the electrode needs to be reconfigured in a single channel data acquisition system, which is both time consuming and laborious. Newer equipment has multiple channels that include multiple electrodes, and measurements are taken through each channel. The SuperSting R8 resistivity meter, produced by Advanced Geosciences, Incorporated, is equipped with eight channels. Therefore, for each current injection, the system utilizes nine electrodes to collect eight different potential difference

measurements (Advanced Geosciences, Incorporated 2006). The variations in the data measurement of single channel and multichannel systems are presented in Figure 2.18.

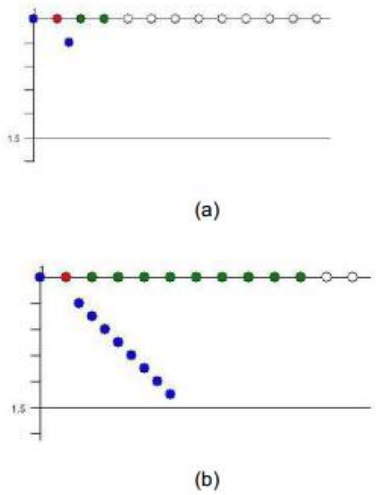

Figure 2.18 (a) Single-channel instrument (SuperSting R1/IP), b. 8-channel Instrument

Multi-channel equipment has to receive instruction on the proper triggering sequence of electrodes. This information can be programmed by manual entry or an uploaded coded command file. The sequencing information considers the array style and the information pertaining to the electrode locations/electrode address during each measuring sequence. There are no theoretical limits to the depth of penetration; however, for tomography applications, practitioners can generally assume that the depth of penetration should be approximately 15 to 25% the size of the object. The electrode spacing should not be greater than twice the size of the object or feature to be imaged. The design of the survey (i.e. survey run length, electrode spacing, and array type) directly impacts the depth of penetration and resolution (Advanced Geosciences Incorporated 2006). For continuous profiling, the roll-along survey technique can be utilized to continuously profile the subsurface along a common survey line. Figure 2.19 presents both two-and-three-dimensional roll-along patterns. As shown, a segment of electrodes is

detached from the original survey line and relocated to the end of the cable system, effectively advancing the survey along the desired imaging path. As the entire line will not be advanced, not all of the reading will be new. In Figure 2.19 (a), the overlapping triangular patterns represent the respective field data points or pseudosection generated during each survey. Based on the instrument and survey design, these readings may either be repeated or disregarded after acknowledging that the measurement has already been done. By using multiple cables, the amount of data overlap is reduced, and more of the survey can be performed with fewer movements. However, a decrease in data overlap will increase the void left below the two overlapping pseudosections, as presented in Figure 2.19 (a) (Advanced Geosciences Incorporated, 2006).

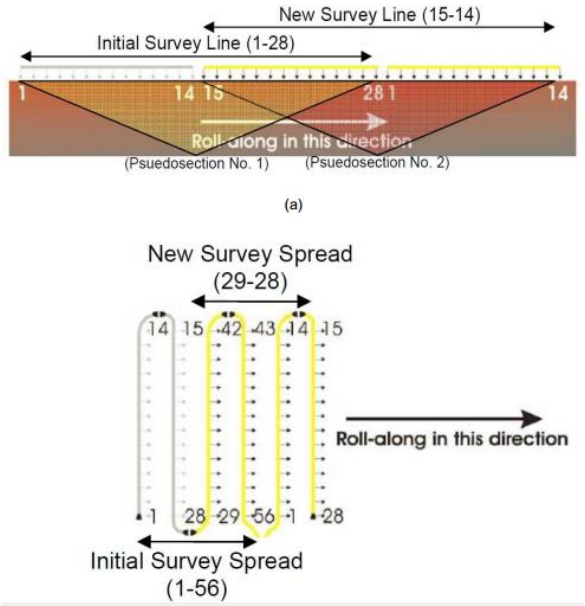

Figure 2.19 Example of a roll-along for (a) Two-dimensional survey (b) Three-dimensional survey

2.5.5 Data Interpretation

The results of resistivity imaging are converted to a visual representation for analysis. Apparent resistivity is calculated from the geometric factor that depends on the

spacing of the current and potential electrodes, potential difference, and injected current. It does not provide the true resistivity and shapes of the anomalies. Mapping apparent resistivity values creates a profile which is known as a pseudosection (Hubbard J. L., 2009). Pseudosections provide a crude representation of the environment surveyed. The apparent resistivity plot in a pseudosection distorts the real subsurface model picture (Samouëlian et al., 2004); however, it can be used to estimate the true subsurface condition. An apparent resistivity pseudosection provides data necessary to complete an iterative inversion process. The purpose of the inversion is to produce a representative earth model pseudosection. During the inversion process, iteration is performed until the modeled pseudosection approaches convergence with the measured pseudosection. The convergence criterion is usually predetermined tolerance for calculated error between the measured and modeled resistivity. The inversion process is best performed using numerical analysis software due to the quantity of data involved and iterative processes. Software packages RES2DINV, RES3DINV and Earth Imager 1D, 2D, and 3D are examples of products available for inversion processing and inversion (Hubbard J. L., 2009). A generalized flow chart for the inversion process is presented in Figure 4.20.

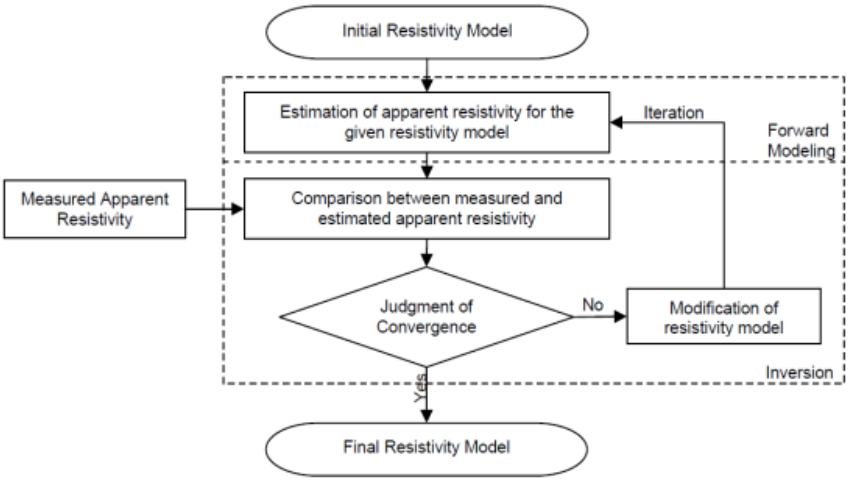

Figure 2.20 Flow Chart of Resistivity Inversion process (Hubbard J. L., 2009).

Chapter 3

TEST METHODOLOGY

3.1 Introduction

The objective of this study was to evaluate root length, using electrical resistivity imaging, in an evapotranspiration (ET) cover. To meet this objective, 2D resistivity imaging was performed on two slopes owned by the City of Irving Landfill in Irving, Texas. The slopes were covered with evapotranspiration cover soil. An extensive laboratory experimental program was developed to investigate the geotechnical properties of the two cover soils, and it was determined that the geotechnical properties of the two cover soils were different enough to assure the effectiveness of resistivity imaging in determining unknown root depths in different types of ET cover soil.

3.2 Study Area Selection

The area selected for this study is part of the City of Irving Landfill, which received permission to start operation in December of 1980 and began operation in April of 1981. Approximately 800 tons of waste are sent to the landfill every day. The waste footprint for the landfill is 139.5 acres, and the disposal capacity of the landfill is 21,290,457 cubic yards. The landfill is divided into tracts which the City identifies as East, West and Middle tracts. The layout plan of the City of Irving Landfill is shown in Figure 3.1.

In the West Tract, there are two slopes, known as the West Slope and the North Slope. They are two of the oldest final covers in the City of Irving Landfill and are covered with native soil and vegetated with Bermuda grass. These two slopes were selected as the study area for this research and are identified as Slope 1 (West Slope) and Slope 2 (North Slope). Slope 1 is located beside Luper Road, and Slope 2 is located beside Hunter Ferrel Road. A survey of the study area was conducted, and the layout of each side slope was measured. The slopes for the study are identified in Figure 3.2.

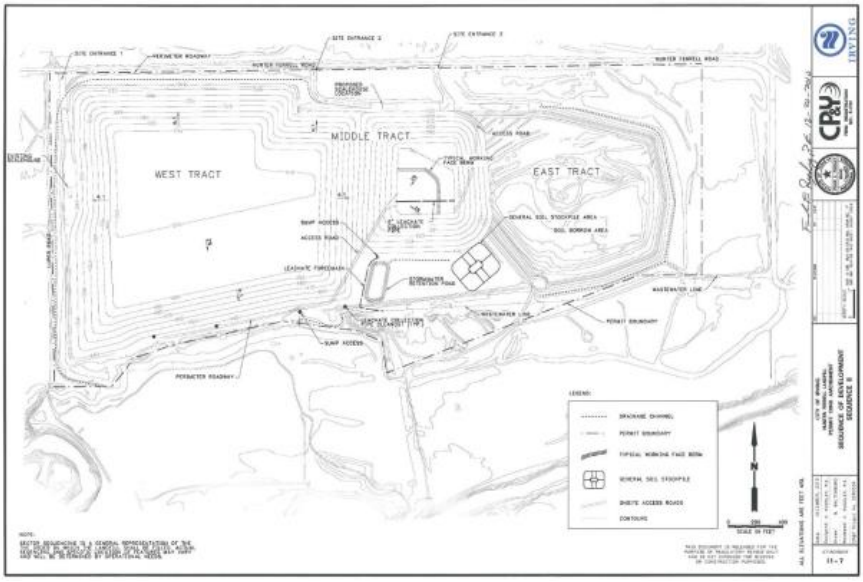

Figure 3.1 Layout of City of Irving Landfill

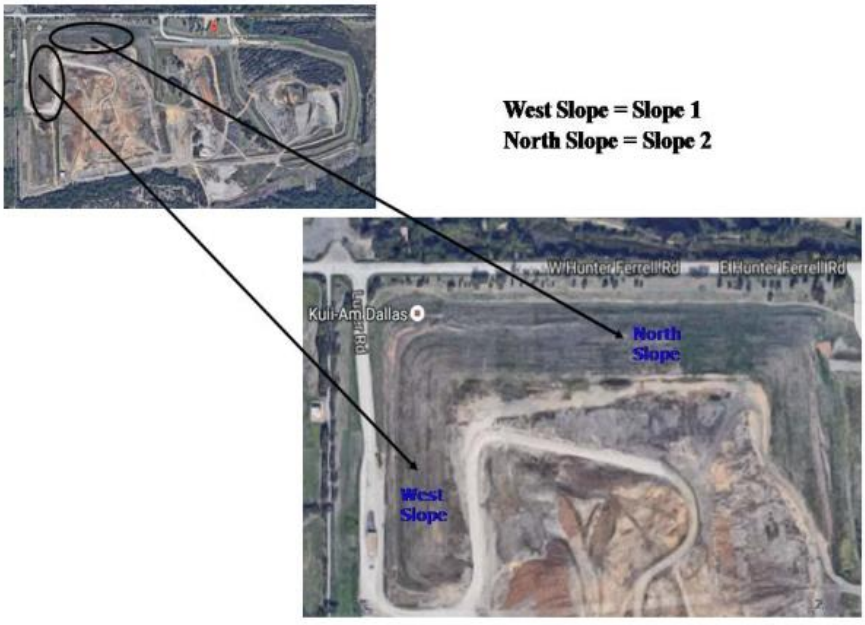

Figure 3.2 Identification of study area

3.3 Collection of Soil Samples and Determination of Geotechnical Properties

Soil samples were collected from Slope 1 and Slope 2 for the determination of geotechnical characteristics. Soil samples for the first phase were collected in June, 2016; samples for the second phase were collected in June, 2017. For each collection phase, four 20-liter buckets of soil samples were collected from each slope (Figure 3.3) and taken to laboratory to determine the geotechnical properties of the soil.

(a) (b)

Figure 3.3 (a) Excavation of soil sample from side Slope 1 (b) Collection of soil sample

3.3.1 Geotechnical Properties of soil

An experimental program was developed to determine the geotechnical properties of the soil specimens. Geotechnical investigations performed on the soil specimens are summarized in Table 3-1.

Table 3-1 Experimental test program on the soil samples

Name of test	**Test Method**
Grain size distribution	ASTM D 422-63
Specific gravity	ASTM D 854-00
Atterberg limits	ASTM D 4318
Moisture density relation	ASTM D 698

3.3.1.1 Grain Size Distribution

Particle size distribution of the samples was determined per the ASTM D422-63 standard test method. (Figure 3.4). The soil samples were oven dried at a temperature of 100-110 °C for 24 hours. The soil aggregate of the oven-dried samples was broken by a mortar-and-rubber-covered pestle, and an approximate 500 gm sample was measured for the sieve analysis. The soil sample was subjected to wet sieving, using a #200 sieve with flowing water, until the leached water was completely clean. The retained and leached samples were dried in the oven at 100-110 °C for 24 hours or until they reached a constant weight. After that, the retained soils were sieved, using #4, #10, #30, #40, #60, #100, and #200 US standard sieves. The mass of retained samples in each sieve was determined after completion of the test. The soil passed through the #200 sieve during wash sieving was utilized in the hydrometer test.

(a) (b) (c)

Figure 3.4 Grain size analysis: (a) Crushing the oven-dried sample, (b) Sieve analysis, (c) Hydrometer analysis

3.3.1.2 Atterberg limits

Atterberg limit tests were performed on the soil specimens per the ASTM D4318 standard method. Samples passing through #40 sieve were considered in the test. After the addition of water, the soil sample was chopped, stirred, and kneaded repeatedly until it became a uniform soil paste. A portion of the soil was placed in the Cassagrande liquid limit device, and a groove was cut at the center of the cup. The cup of the device was lifted

and dropped at a rate of 2 drops/second until the groove was around 10 mm. The test was repeated four times, and the number of blows was plotted against the moisture content. The moisture content corresponding to 25 blows was considered as the liquid limit of the specimen. For the determination of the plastic limit, water was added to the soil and kneaded repeatedly. The soil masses were rolled in the glass plate until threads of about 3 mm were formed. When the threads were broken at 3 mm diameter, they were put in the moisture cans. Samples were dried in the oven at 100-110 °C for 24 hours or until constant weight was gained. The moisture content at this condition was considered as the plastic limit of the specimen.

3.3.1.3 Moisture Density Relation

The Standard Proctor Compaction Test was conducted on the collected soil samples, following the ASTM 698 Standard method. Soil samples collected from different lysimeters were oven dried for 24 hours. After drying, the samples were crushed and pulverized. The pulverized samples were then used for the Proctor test to determine the optimum moisture content (OMC) and maximum dry density (MDD), and to evaluate the dry side and wet side of the compaction curve.

Figure 3.5 Standard Proctor Compaction Test

3.3.1.4 Specific Gravity

Specific gravity of the collected soil samples was measured according to ASTM D 854-00 standard test method. Approximately 50 gm of soil mass were weighed after passing through a #10 sieve. After weighing the empty pycnometer and the pycnometer with the soil specimen, distilled water was added to the specimen. A partial vacuum was also applied to the soil for 16 to 24 hours to remove the air bubbles. Then water was added to the pycnometer up to the desired level, and the weight was measured. Distilled water was then added to the clean pycnometer, and the weight was re-measured.

3.3 Subsurface Imaging of Vegetation by Electrical Resistivity

Resistivity of a shallow subsurface is determined by resistivity imaging. A SuperSting R8/IP resistivity meter was used during the field investigation. The SuperSting is a multichannel system which consists of 8 channels for conducting surveys. There are 8 receivers in the 8-channel system, and it takes 8 readings per current injection, making it 8 times faster than single-channel system. A maximum of 56 electrodes can be used in this multichannel system, but 28 electrodes can also be used, depending on the site condition. The system allows variable electrode spacing, with a maximum distance of 20 feet between two adjacent electrodes. It includes a SuperSting R8/IP resistivity meter, switch box, electrodes, cables, and a 12-volt battery. The switch box is built in and is available for 28 or 56 electrodes. It is used with passive cables and electrodes to form a central switching system. The RI test setup, using the SuperSting R8/IP resistivity meter, is presented in Figure 3.6.

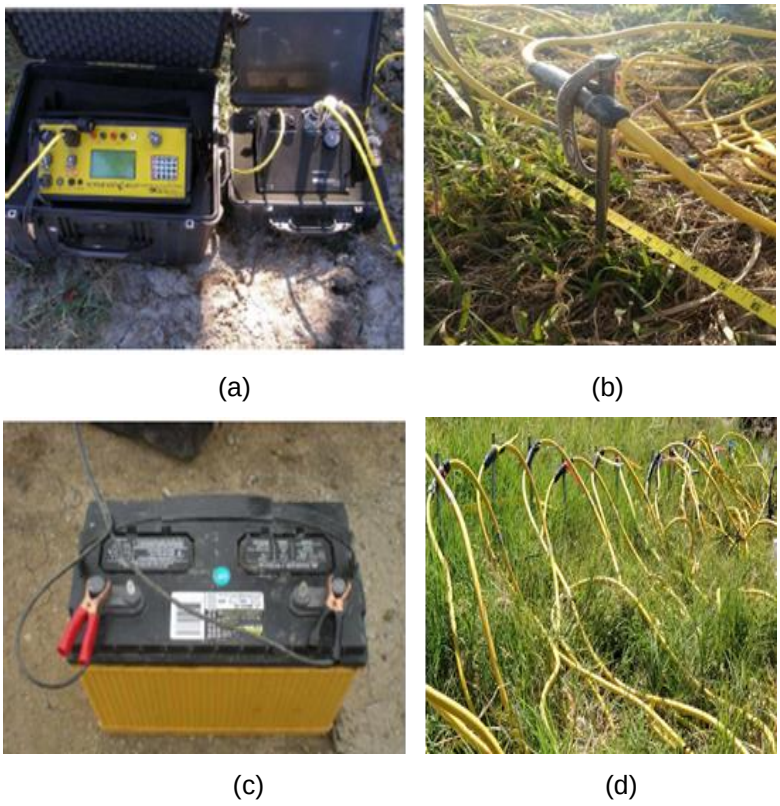

(a) (b)

(c) (d)

Figure 3.6 Resistivity imaging test setup: (a) SuperSting R8/IP resistivity meter with switch box, (b) Electrodes connected with cable, (c) 12-volt power supply, (d) Resistivity line

The electrode spacing required for performing resistivity imaging is dependent on factors such as the quality of resolution desired, penetration depth required, and size of objects under investigation. With smaller electrode spacing, the quality of the resolution improves, but penetration is shallower. For the same number of electrodes, larger electrode spacing leads to deeper penetration. For this study, 2D resistivity imaging was conducted with smaller spacing to get better resolution.

Apparent resistivity data was collected during the RI test and stored in raw form in the SuperSting R8/IP meter. The raw data was converted into a form that would make processing easy after extracting it from the SuperSting R8/IP meter. AGI administrator

software was used to download the data and convert it into a readable format for the AGI EarthImager 2D analysis software. The collected field data was used to plot the apparent resistivity pseudosection, and the inverted resistivity section was re-created by the AGI EarthImager 2D software. The reconstruction of the subsurface resistivity distribution from measured apparent resistivity was done by the process of inversion. EarthImager 2D software allows forward modeling, damped least squares inversion, smooth model inversion, and robust inversion (Advanced Geosciences, Incorporated 2006).

A starting resistivity model is constructed based on either average apparent resistivity or apparent resistivity distribution during the inversion process. A virtual survey or forward modeling is performed for a predicted data set. The initial root mean square (RMS) error is calculated at the zero-th iteration. A linearized inversion is used to update the model, and the model value is adjusted in the finite element mesh. Iteration continues until an acceptable model value for RMS is reached. If an error level remains beyond the acceptable limit, the raw data should be evaluated to see whether it was caused by the outlier measurement inverted model. Data points which are corrupted can be isolated by using a misfit histogram generated in the AGI Earth Imager program. They can also be manually eliminated in the pseudosection or by suppressing readings of particular electrodes. The iteration process can be stopped when the model demonstrates the subsurface condition within the accepted error tolerances for the survey (Advanced Geosciences Incorporated, 2006).

2D RI tests were performed in the two slopes of the Irving Landfill to determine the depths of the roots. Twenty-eight electrodes, spaced one foot apart, were used for each test. The resistivity line was 27 ft. . Figure 3.7 and Figure 3.8 depict the resistivity layout and line positions of the electrodes in the two slopes, respectively.

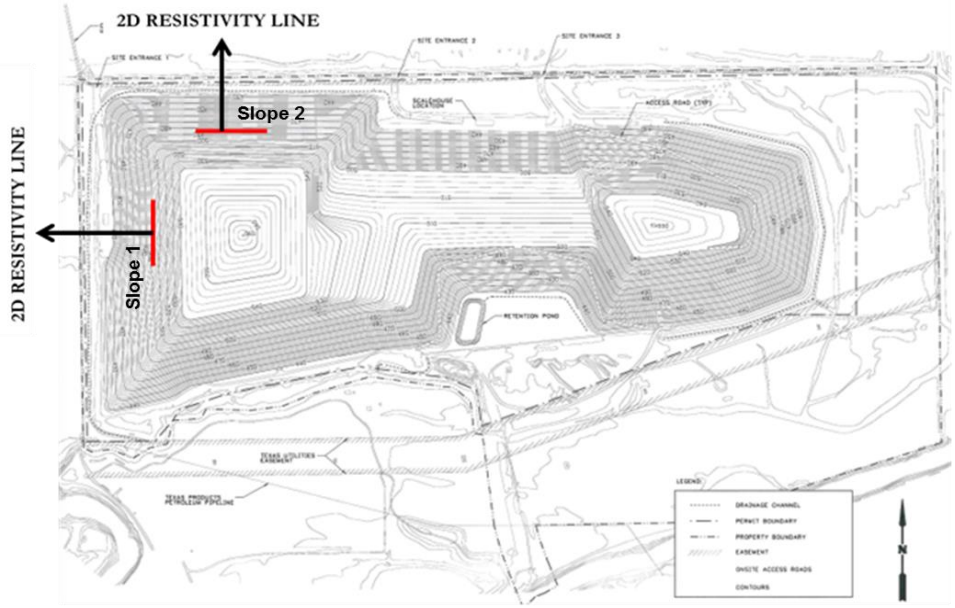

Figure 3.7 Resistivity layout for the two slopes at the City of Irving Landfill

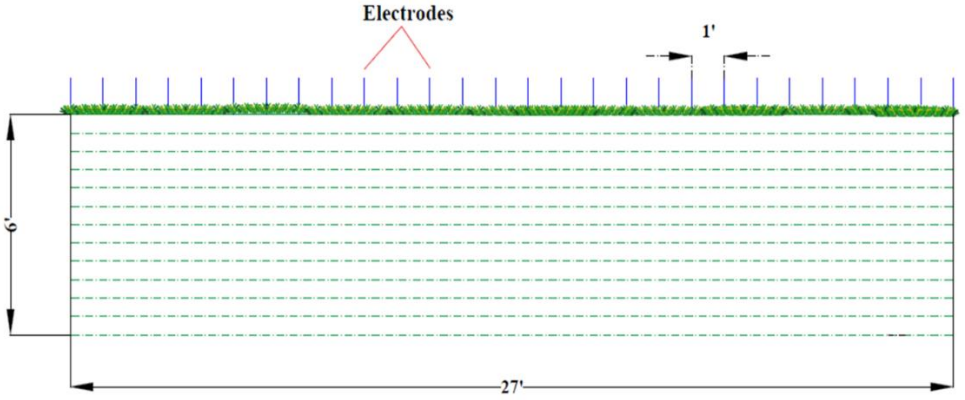

Figure 3.8 Electrode positioning along RI line (Slope 1 and Slope 2)

The resistivity imaging field setup for Slope 1 and Slope 2 is presented in Figure 3.9. The dipole-dipole array was used for both of the tests. The test data was recorded during the field investigation and was transferred to a computer for further analysis.

(a) (b)

Figure 3.9 Resistivity imaging test at the City of Irving Landfill: (a) Slope 1, (b) Slope 2

3.4 Root Zone Observation with Acrylic Tube: Minirhizotrons

Bates (1937) introduced a transparent, hollow, cylindrical tube for use in observing in-situ plant roots behind the tube. Bohm (1974) termed the tubes, as minirhizotrons. Alam (2017) was the first to apply this method (minirhizotron) for a root system study for the evaluation of the performance of ET cover. A 4-foot long, hollow, acrylic plastic tube, with an inside diameter of 6 inches was used for this research.

A pipe with a wall thickness of 1/8 inch was used for this study. The wall thickness of the pipe was very important because optimal thickness was required for clear visibility of the roots, and the pipe had to be strong enough to resist buckling. The pipes were driven 30 inches into the cover soil, with 18 inches kept above the soil surface. Figure 3.11 (a) shows the minirhizotron installed in the field. A motorized spiral augur was used to bore holes of approximately 6-inch diameter vertically to a depth of 2.5 feet (30 inches). To limit the smear, a steel brush was pushed up and down several times after the holes were bored. The minirhizotron (48 inches) was then inserted into the holes and pushed all the way to the bottom. The diameters of the holes were kept slightly higher than the diameters of the minirhizotrons. The parts of the minirhizotrons extending above the soil surface (18

inches) were capped to prevent the intrusion of light and water. To obtain good contact between the outside wall and the soil, in-situ bored soil was used to fill the gap between the hole and the outside wall of the minirhizotron. The root depth was measured and marked on the minirhizotron during its installation. Almost two weeks after the natural

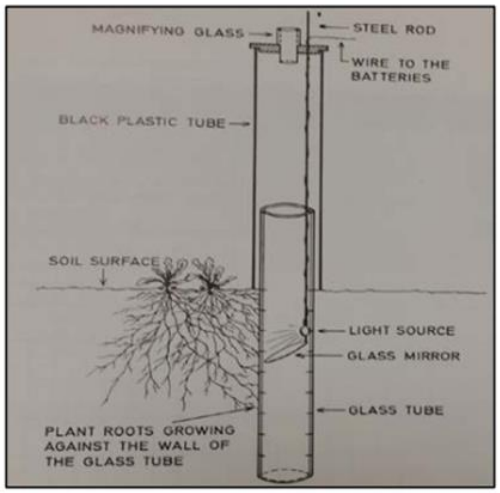

Figure 3.10 Block diagram with the principle of observing root through glass tube (Bohm, 1974)

consolidation of the soil, roots were visible inside the minirhizotron. One or two weeks after the installation of the minirhizotrons, roots were not visible due to the disturbance around the minirhizotrons. However, once the natural consolidation of soil is done after almost two weeks, concentration of roots increased behind the minirhizotron wall. A high-resolution minirhizotron camera (mini camera) was utilized in the current study to view the roots, capture and store the digital images, then transfer them to the computer (Figure 3.11). This mini camera can be rotated 360^{o} in the minirhizotron tube, at any depth.

(a) (b) (c) (d)

(e) (f)

Figure 3.11 In situ image acquisition from minirhizotron: (a) Boring with spiral augur, (b) borehole, (c) inserting plexiglass, (d) installed minirhizotron, (e) setting up camera, (f) image acquisition after plugging into computer

Chapter 4

RESULTS AND DISCUSSION

4.1 Field Investigation Results

The objective of the research was to evaluate plant root length in evapotranspiration (ET) cover soil, using electrical resistivity imaging. 2D Resistivity Imaging (RI) was performed on ET cover soil of the West slope (Slope 1) and North slope (Slope 2) in the City of Irving Landfill, in Irving, Texas to determine the root length of vegetation. Soil characterization was also done to evaluate the properties of the ET cover soil. Laboratory tests were conducted on the collected soil samples to determine the geotechnical properties. The estimated root lengths, found by the electrical resistivity imaging method, was verified by installing acrylic tubes in the field and taking root images from minirhizotrons to quantify root length. An analytical model was also developed to determine root length, based on its relationship with variations of resistivity and precipitation. The test results are presented below.

4.2 Soil Characterization

4.2.1 Grain Size Distribution

The grain size distribution of the soil samples is presented in Figure 4.1. The results are shown from the top soil only. Based on the results from the wet sieving, the fine fraction of the soils from Slope 1 and Slope 2 were approximately 76% and 92% (average of 3 sets of tests), respectively. From the hydrometer test, the clay fraction was found higher than the silt fraction for both the soils. The percent of sand, silt, and clay (based on one test) for the soils is summarized in Table 4-1.

Table 4-1 Sand, silt, and clay fractions

Fraction	Slope 1	Slope 2
Sand	24.54%	7.19%
Clay	57.75%	77.5%
Silt	19.52%	13.86%

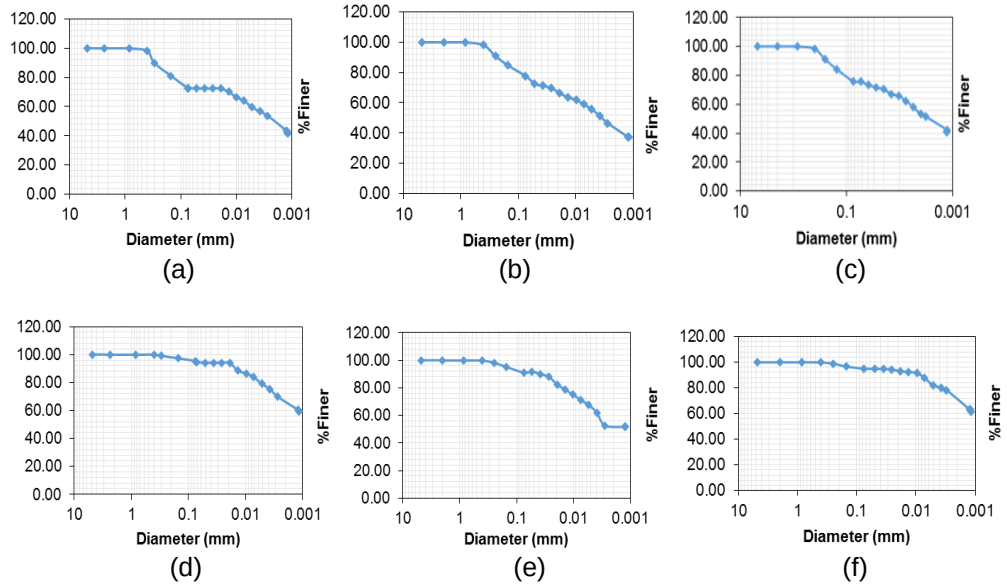

Figure 4.1 Grain size distribution curves for soils of two slopes: (a) Slope 1 (Trial 1), (b) Slope 1 (Trial 2), (c) Slope 1 (Trial 3), (d) Slope 2 (Trial 1), (e) Slope 2 (Trial 2), (f) Slope 2 (Trial 3)

4.2.2 Atterberg Limits

The measured liquid limits and plasticity indices of the soil samples collected from Slope 1 were between 46 and 51, and 21 and 23, respectively (Figure 3.6). The measured liquid limits and plasticity indices of the soil samples collected from Slope 2 were between 64 and 69, and 34 and 36, respectively (Figure 4.2). Based on the sieve analysis and Atterberg limit test results, soil from Slope 1 was classified as low plastic clay (CL) and

from Slope 2 was classified as high plastic clay (CH) as per the Unified Soil Classification System (USCS).

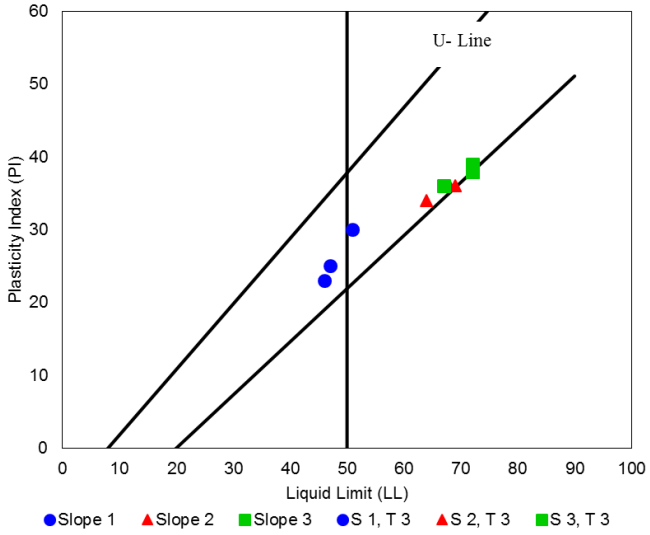

Figure 4.2 Plasticity chart for ET cover soil

4.2.3 Specific Gravity

Specific gravity of the collected soil samples was determined in accordance with the ASTM standards. The specific gravity of the soil samples of Slope 1 was 2.7 and Slope 2 was 2.69.

4.2.4 Moisture Density Relation

Standard Proctor compaction tests were conducted on the collected soil specimens the two slopes. Based on the results, the optimum moisture content (OMC) of the cover soil of Slope 1 ranged from 13% to 16%, and the max dry density (MDD) was from 111 to 114 pcf for three different tests (Figure 3.7). The OMC of the cover soil of Slope 2 ranged from 21% to 22%, and the MDD was from 99 to 102 pcf for three different tests. The compaction curves for the top soil of both slopes are shown in Figure 4.3.

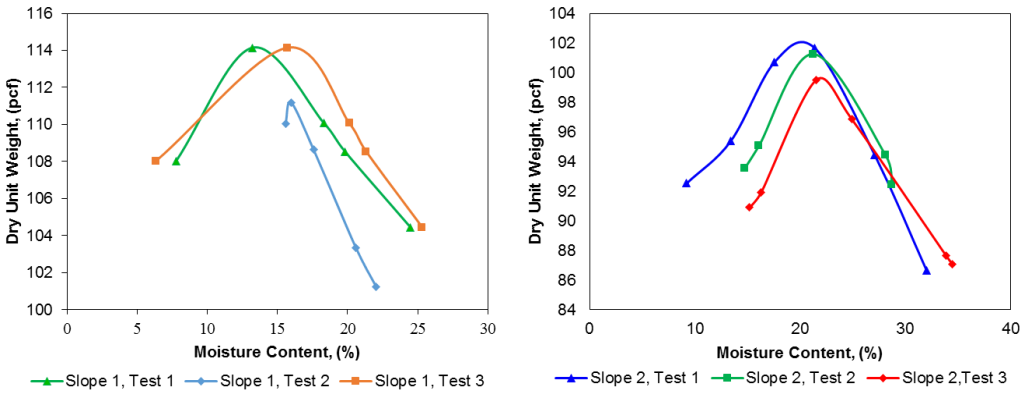

Figure 4.3 Compaction curves of Slope 1 and Slope 2

4.3 Soil Resistivity

ERI is an active geophysical method which measures the electric potential differences at specific locations by injecting a controlled electric current at other locations. The theory is that in an entirely homogeneous half-space, a resistivity value can be calculated for the subsurface by knowing the current injected and measuring the resulting electric potential at specific locations (Ahmed et al. 2018). 2D resistivity imaging (RI) test was performed at the West slope (Slope 1) and North Slope (Slope 2) of the City of Irving Landfill to determine the root length of the vegetation. The investigation was conducted throughout the year 2017 in both slopes.

4.3.1 Resistivity Imaging profiles

An electrical resistivity test was done by placing 28 electrodes at 1 foot intervals in the ET covers of Slope 1 and Slope 2 of the City of Irving Landfill. The 2D RI test gave the inverted resistivity imaging profile up to a maximum depth of approximately 6.53 feet vertically. Based on the field investigation, the inverted resistivity pseudosection for Slope 1 and Slope 2 is presented in Figure 4.4 and Figure 4.5 below.

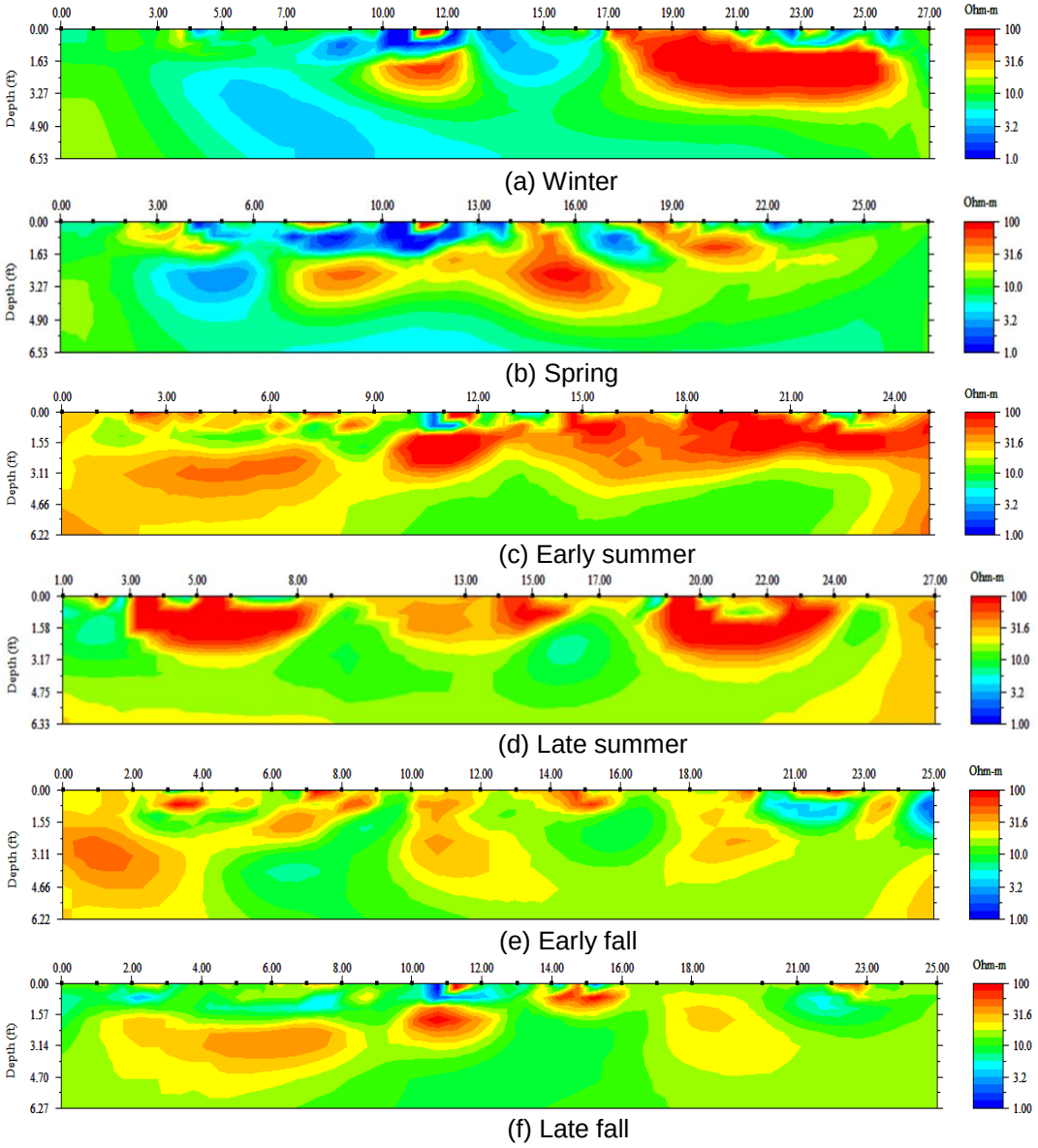

Figure 4.4 Electrical resistivity imaging profile for Slope 1: (a) Winter (20th January, 2017), (b) Spring (3rd March, 2017), (c) Early summer (9th May, 2017), (d) Late summer (18th August, 2017), (e) Early fall (9th September, 2017), (f) Late fall (27th November, 2017)

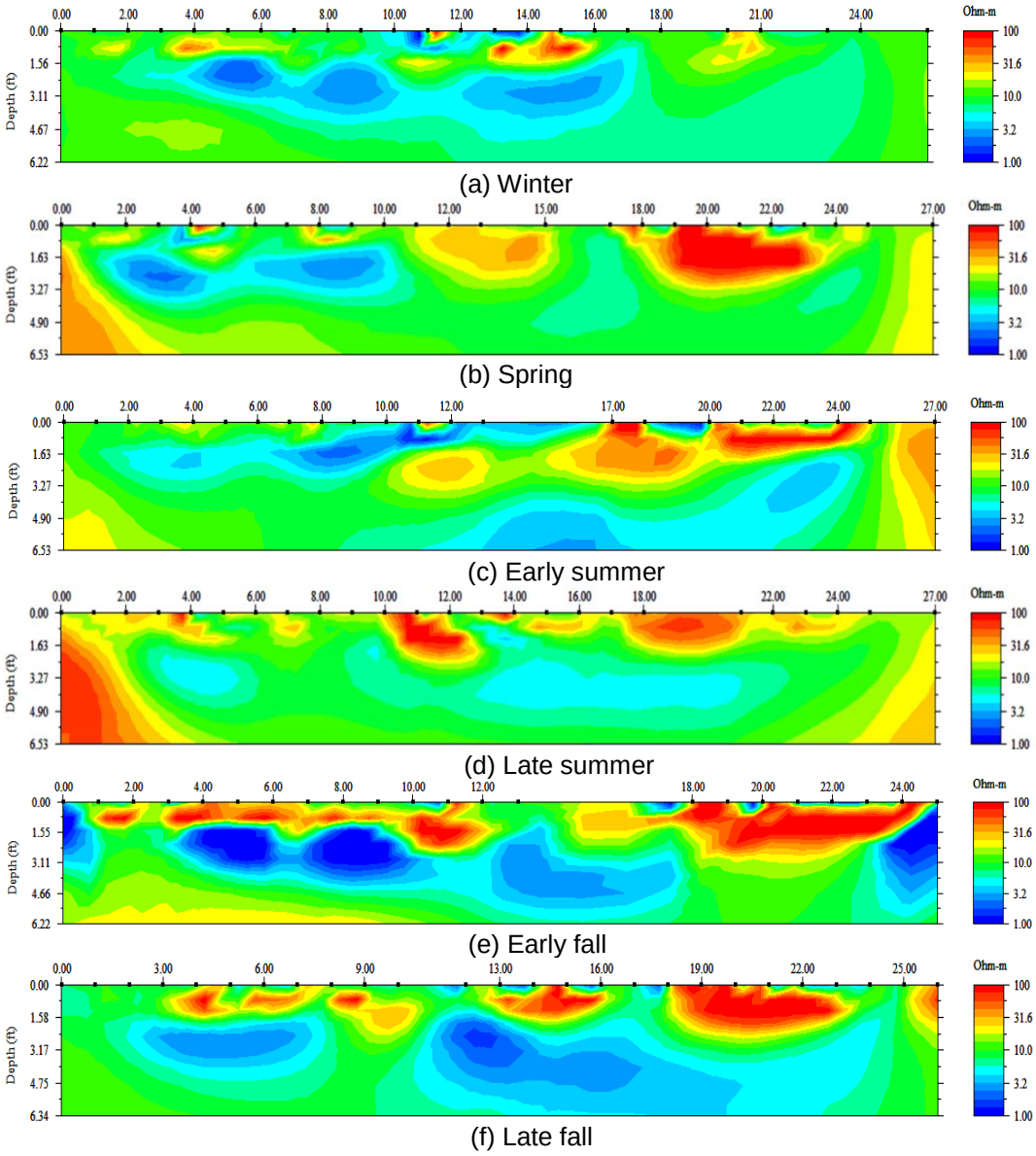

Figure 4.5 Electrical resistivity imaging profile for Slope 2: (a) Winter (20th January, 2017), (b) Spring (3rd March, 2017), (c) Early summer (9th May, 2017), (d) Late summer (18th August, 2017), (e) Early fall (9th September, 2017), (f) Late fall (27th November, 2017)

Resistivity data sets are presented, using a dipole-dipole configuration and spanning a full cycle of seasons. The scale from red to blue in Figure 4.4 and Figure 4.5 indicates levels of high and low resistivity values, respectively. For Slope 1, high resistivity was observed within the top 1.5 feet to 2 feet of the resistivity imaging profiles (Figure 4.4). Beneath this depth, the resistivity imaging profile showed comparatively low resistivity. For Slope 2, high resistivity was found in the top 1 foot to 1.5 feet of the imaging profiles (Figure 4.5). The imaging profiles also depict much less variation of resistivity at deeper depths.

4.3.2 Data extraction from 2D RI profiles

Twenty-eight (28) electrodes, spaced 1 ft. apart and covering a maximum vertical depth of approximately 6.53 ft., were utilized in the current study to conduct the resistivity test. For uniformity of analysis, data was extracted to a depth of 6 feet in the vertical direction from the RI profile for each season. Vertical sections were made in the RI profiles at every 0.5 foot interval of soil transect; the resistivity data was extracted along these vertical sections. Since the RI profiles were 27 feet long horizontally, there were 53 sections available for data extraction. The data extraction sections under consideration are shown in Figure 4.6.

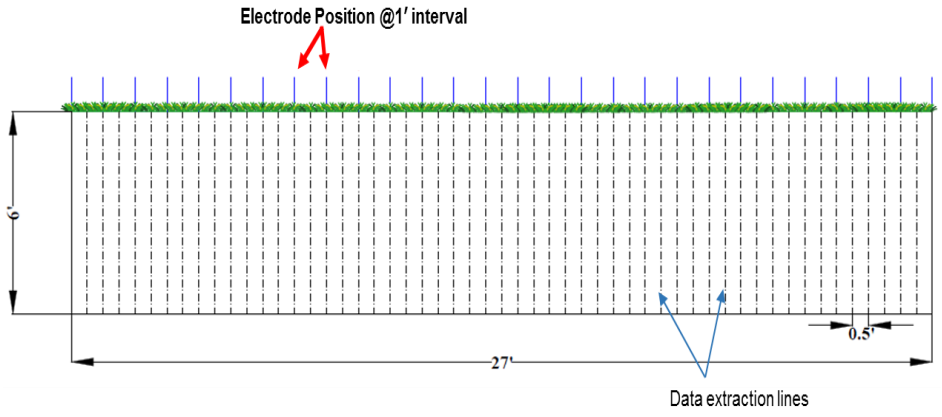

Figure 4.6 Extraction of data along soil transect of RI profile (at every 0.5 foot interval in horizontal direction)

4.4 2D RI Data Analysis

2D RI data was extracted from resistivity imaging profiles of Slope 1 and Slope 2 of the City of Irving Landfill. The data was plotted against depth for each season. For a particular depth, the average resistivity of 53 sections along the soil transect was taken into consideration for analysis (Figure 4.6). The average resistivity at different depths reduced the possibility of the over prediction or under prediction of a resistivity value at a particular point. The variations of resistivity with depth in each season for Slope 1 and Slope 2 are presented in Figure 4.7 and Figure 4.8, respectively. The plots revealed that the resistivity decreases after a certain depth. From the spatial distribution of Slope 1 (Figure 4.7) and Slope 2 (Figure 4.8), it was seen that a comparatively higher resistivity band prevailed within a depth of 1 foot to 2.5 feet from the soil surface. Beneath these depths, the electrical resistivity value of the soil decreased. In most cases, a drastic reduction in soil resistivity value was seen after a certain depth.

The top soil of both slopes experienced the highest values of resistivity, mostly because of the presence of roots. Beneath the top soil, the resistivity values started decreasing, and decreased almost uniformly. Soil volumes colonized by roots show high resistivity (Paglis, 2013); therefore, the ability to detect roots depends on the high resistivity of roots compared with soil materials and other soil features (Amato et al., 2008). Values of electrical resistivity below rooted soil layers are mostly related to intrinsic soil characteristics rather than to the presence of roots (Paglis, 2013).

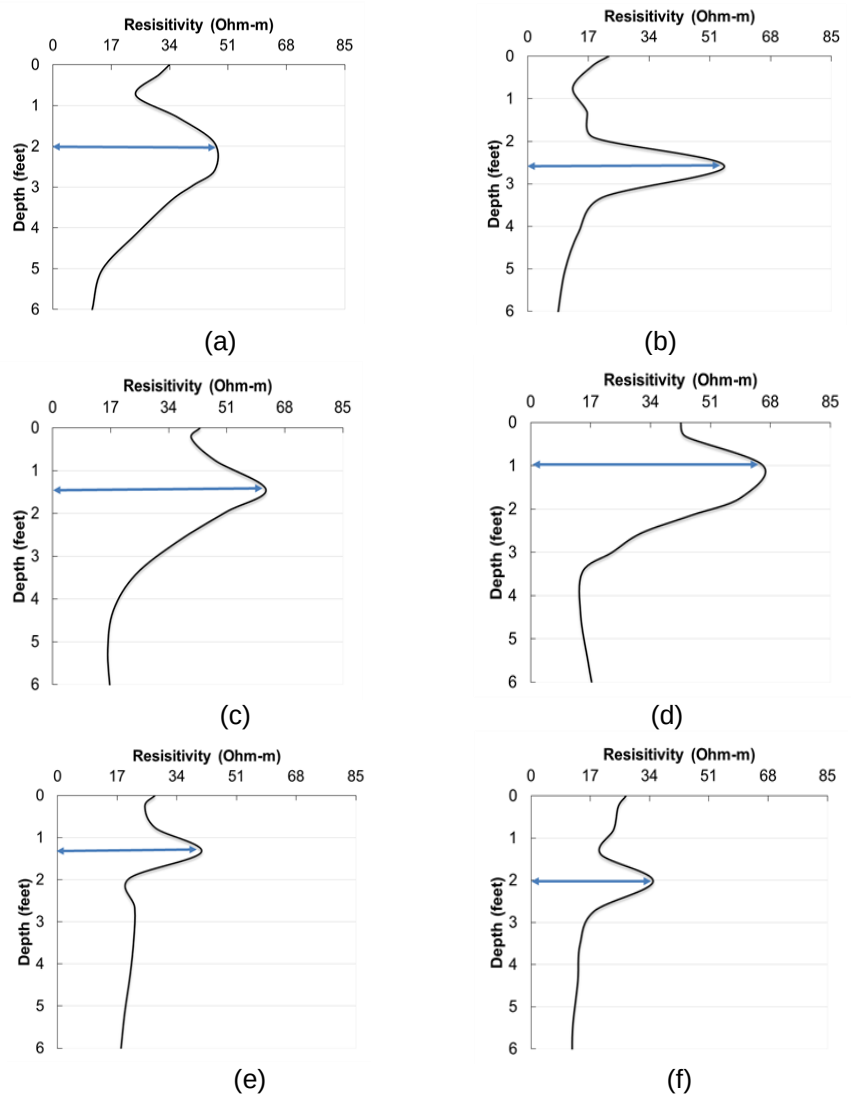

Figure 4.7 Variations of soil resistivity along depth for Slope 1: (a) Winter (20th January, 2017), (b) Spring (3rd March, 2017), (c) Early summer (9th May, 2017), (d) Late summer (18th August, 2017), (e) Early fall (9th September, 2017), (f) Late Fall (27th November, 2017).

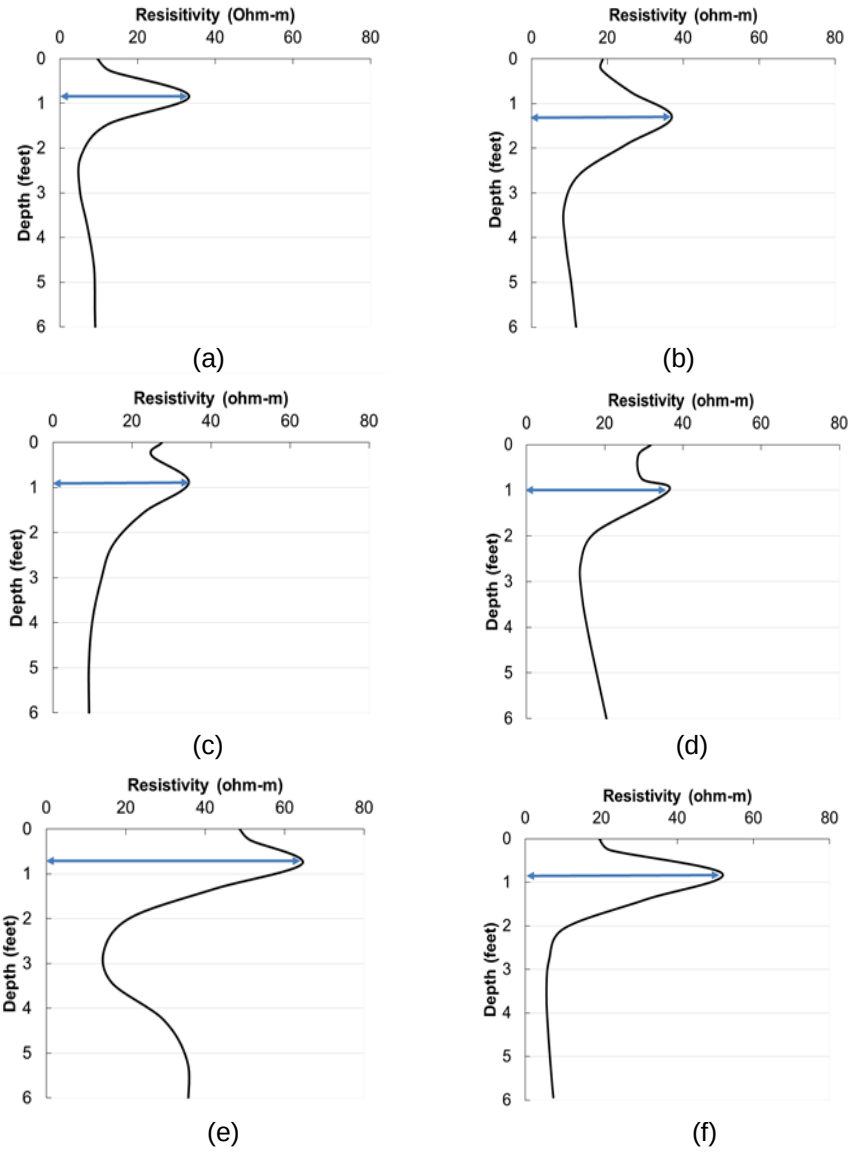

Figure 4.8 Variations of soil resistivity along depth for Slope 2: (a) Winter (20th January, 2017), (b) Spring (3rd March, 2017), (c) Early summer (9th May, 2017), (d) Late summer (18th August, 2017), (e) Early fall (9th September, 2017), (f) Late fall (27th November, 2017)

In the studied soil transects, the higher resistivity values were dominated by the presence of roots. The resistivity value of top soil is mostly influenced by seasonal variations of plant root dynamics. Ecologists describe root activity as periodic, as the number of total roots, living roots and new roots significantly vary from season to season (Sun et al., 2011). Since moisture in the ET cover is transpired through vegetation, the seasonal variations in the root dynamics pattern affect moisture content in the ET cover. Given the relationship between resistivity and moisture content, the seasonal effect on moisture content affects soil resistivity (Ahmed et al., 2017). Root zone soil resistivity is largely influenced by variations of evapotranspiration due to seasonal differences (Jayawickreme, Dushmantha H., 2008). The effect of the seasonal root dynamics pattern in this study was reflected in extracted resistivity values when plotted against depth of soil mass (Figure 4.7 and Figure 4.8).

A dilemma arose in determining active root zone depth in this study since the plotting in Figure 4.7 and Figure 4.8 showed varying high resistivity zones in different seasons for both slopes. The depth of the high resistivity soil layer was noted for every season during 2017, and Tables 4-2 and 4-3 show that the mean resistivity plot against depth for the noted six seasons did not provide any identical high resistivity zones over the year 2017.

Table 4-2 Depth of high resistivity zones for Slope 1

Season	**Depth of high resistivity zone (feet)**
Winter	2
Spring	2.585
Early summer	1.442
Late summer	1
Early fall	1.342
Late fall	2.025

Table 4-3 Depth of high resistivity zones for Slope 1

Season	Depth of high resistivity zone (feet)
Winter	0.843
Spring	1.301
Early summer	0.886
Late summer	1
Early fall	0.78
Late fall	0.85

4.4.1 Estimation of Root Length

In the process of extracting data from the RI profile, the resistivity profile was divided into 53 sections, with 0.5 foot intervals, in a horizontal direction (Figure 4.6), and the individual sections were then brought under consideration for better representation of the active root zone. The depth at which a drop in resistivity initiated was noted for each section for every season, as was the frequency of the drop.For a particular depth, frequency of resistivity drop at that depth was noted. For example, in Figure 4.9 (a), in 16 out of 53 sections, after 1 foot of depth, the resistivity value started to decrease. Thus, the frequency of “1 foot” depth was noted as 16. The RI profiles for these 16 cases are shown in Figure 4.9 (b), which also shows that the soil resistivity value decreased after 1 foot of depth. Some sections had similar resistivity values along the total depth. Sections having no noticeable change in resistivity along depth were ignored from analysis.

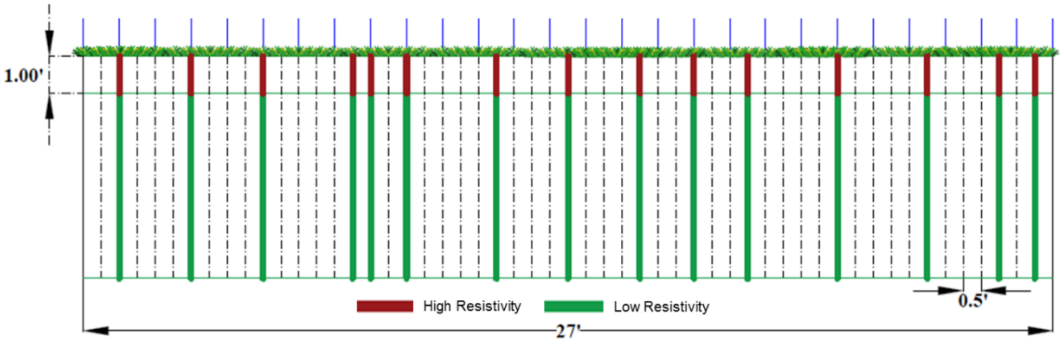

(a)

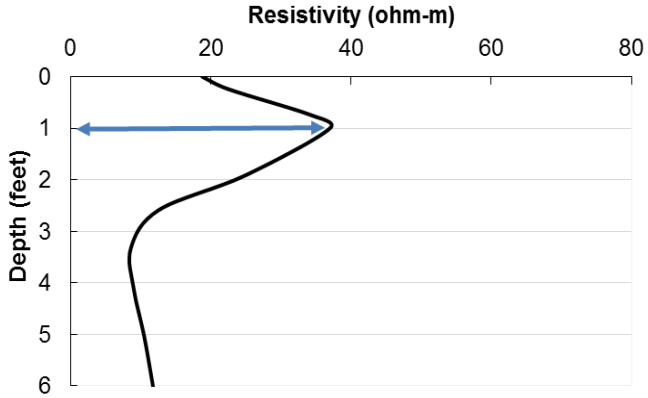

(b)

Figure 4.9 Estimation of effective root depth: (a) Schematic for frequency selection of high resistivity depth, (b) Resistivity distribution

The plotted data (frequency plot) produced normal distribution (Figure 4.10 and Figure 4.11). In a normal distribution curve, most of the data is centered around the mean. The “mean” of a normal distribution curve is the highest number of occurrences of an event. The important thing to note about a normal distribution is that the curve is concentrated in the center and decreases on both sides. This is significant in that the data has less of a tendency to produce unusually extreme values, called outliers.

For the estimation of the active root zone, the maximum and minimum values from the normal distribution curve were ignored. As moved farther out, on either side of the

mean, fewer values represented depths with high resistivity. This means that the higher resistivity distribution was significantly less on the depths lying on either side of the mean. For determining effective rooting depth, it signifies that the root zone mainly lies around the mean of the distribution.

Based on the analysis, the estimated active root zone or root length for Slope 1 was the mean of the data set, 1.865 feet or 1.9 feet (Figure 4.10). Up to a depth of 1.9 feet, a comparatively high resistivity existed in Slope 1 throughout 2017. The estimated active root zone for Slope 2 was the mean of the data set, 1.2 feet (Figure 4.11), signifying that up to a depth of 1.2 feet from the cover surface, high resistivity prevailed throughout 2017.

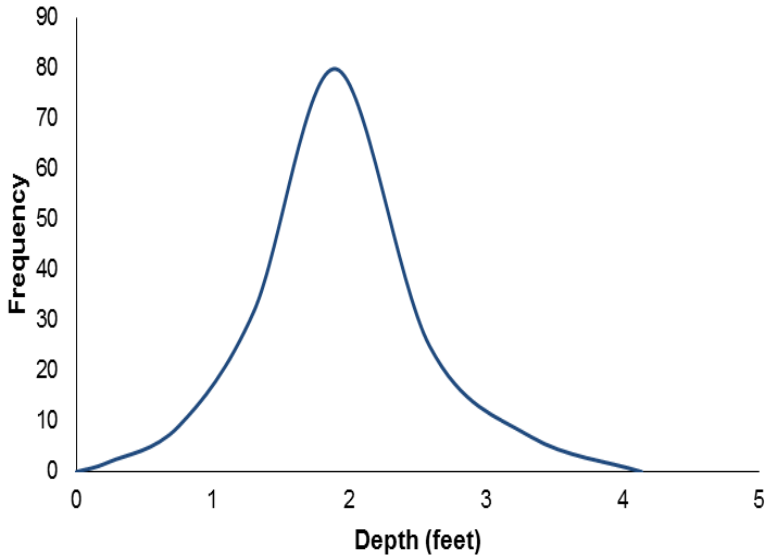

Figure 4.10 Normal distribution curve for high resistivity zone of Slope 1

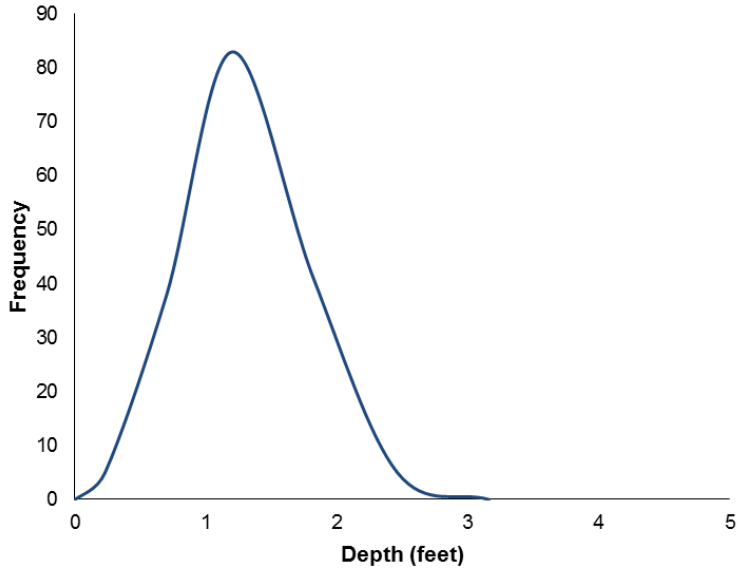

Figure 4.11 Normal distribution curve for high resistivity zone of Slope 2

The normal distribution curves depicted in Figure 4.10 and Figure 4.11 show that high resistivity prevailed up to a depth of 1.9 feet and 1.2 feet in Slope 1 and Slope 2, respectively, throughout 2017.

The cover soil can be divided into two layers: top soil layer and bottom soil layer. The top soil layer of Slope 1 was up to 1.9 feet from soil surface, and the bottom layer was 4.1 feet beneath the top layer. For Slope 2, the top layer was up to 1.2 feet from the soil surface, and the bottom layer was 4.8 feet beneath the top layer. Statistical properties of the soil resistivity for the two layers are given in Table 4-4, which shows that the range of soil resistivity values in the bottom soil layer was pretty small compared to that of the top soil layer in both slopes. The small standard deviation in resistivity values of the bottom layers signified that the resistivity values in the data set of the bottom layer, on average, were closer to the mean of the data set. Similarly, a comparatively large standard deviation in the top soil layer means that the resistivity values in the data set are farther away from

the mean, on average. Plots of the resistivity distribution of the top and bottom soil layers of the ET cover for both Slope 1 and Slope 2 are shown in Figure 4 12.

Table 4-4 Statistical properties of resistivity values

	Rooted zone		Non-rooted zone	
Properties	Slope 1	Slope 2	Slope 1	Slope 2
Mean	36.60799	29.96611	14.9763	11.26997
Standard Deviation	29.36592281	27.61294	8.998032	7.704504
Minimum	1.049	1	0	1
Maximum	100	100	44.891	39.856

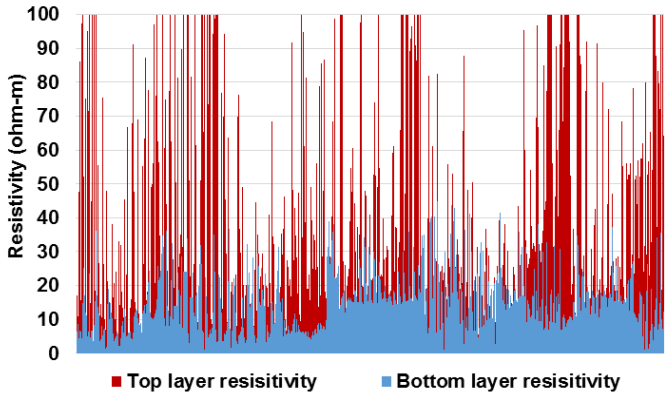

(a)

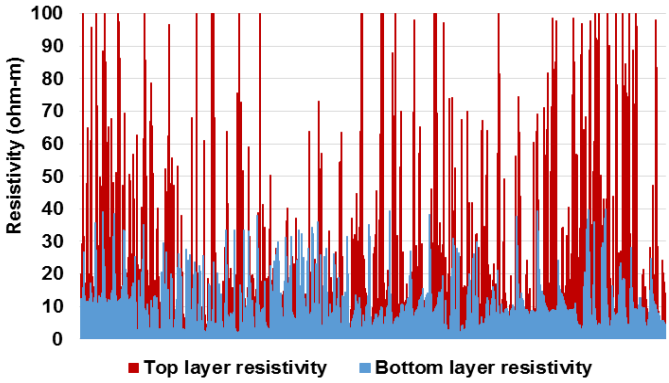

(b)

Figure 4.12 Distribution of resistivity values (a) Slope 1, (b) Slope 2

Figure 4 12 shows the spatial variability in the electrical resistivity along the soil profile. The variability was more evident in the top layers in the studied transect; the variability of the deep soil layers was much lower.

Roots are more concentrated in the top layer of the soil, and the disturbance and variability in electrical resistivity values observed at the top soil layer can be attributed to the presence of roots (Paglis, 2013). The spatial variability in the top soil layer reflects the spatial distribution of roots. Roots remain clustered in some positions within the soil mass (Paglis, 2013). Clustered and non-clustered positioning of roots produces higher variability in resistivity values in the top soil layer. The small variability in the bottom soil layer might be more related to intrinsic soil factors, by its natural condition rather than by the presence of roots. Based on this investigation, it can be estimated that the root length for Slope 1 was 1.9 feet; for Slope 2, the root length was 1.2 feet. Schematics of the root zones for Slope 1 and Slope 2 are in shown in Figure 4.13 and Figure 4.14, respectively.

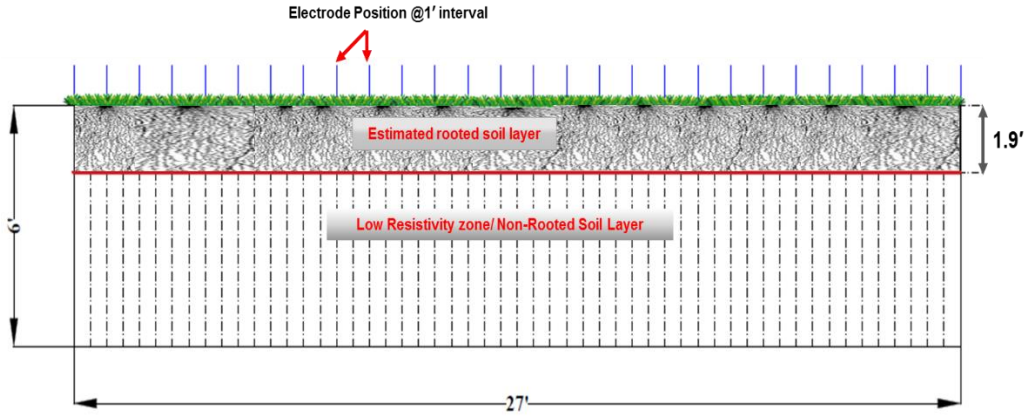

Figure 4.13 Schematic of root zone for Slope 1

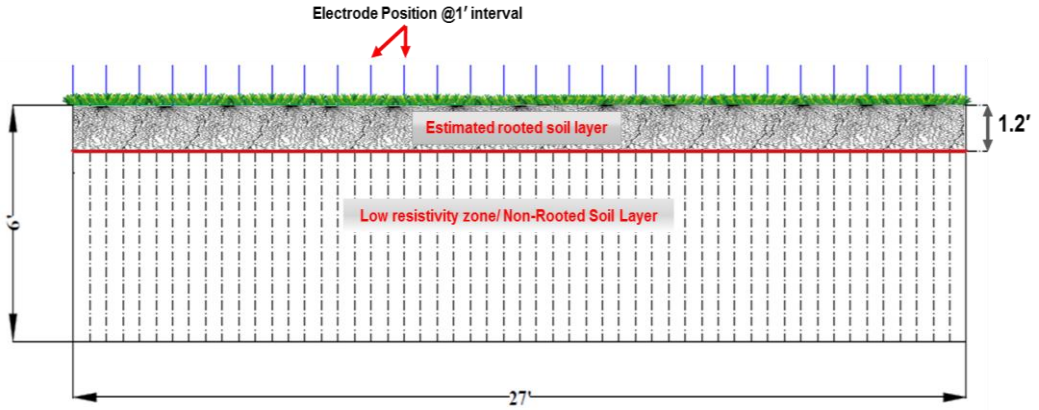

Figure 4.14 Schematic of root zone for Slope 2

4.4.2 Variation of Resistivity with Precipitation

The extracted resistivity data was plotted against the amount of precipitation. Figure 4.15 and Figure 4.16 show the variation of mean resistivity with precipitation for Slope 1 and Slope 2. The mean resistivity fluctuated with variations of precipitation up to 1.9 feet and 1.2 feet for Slope 1 and Slope 2 respectively. The mean resistivity line beneath this depth showed very negligible variation with precipitation.

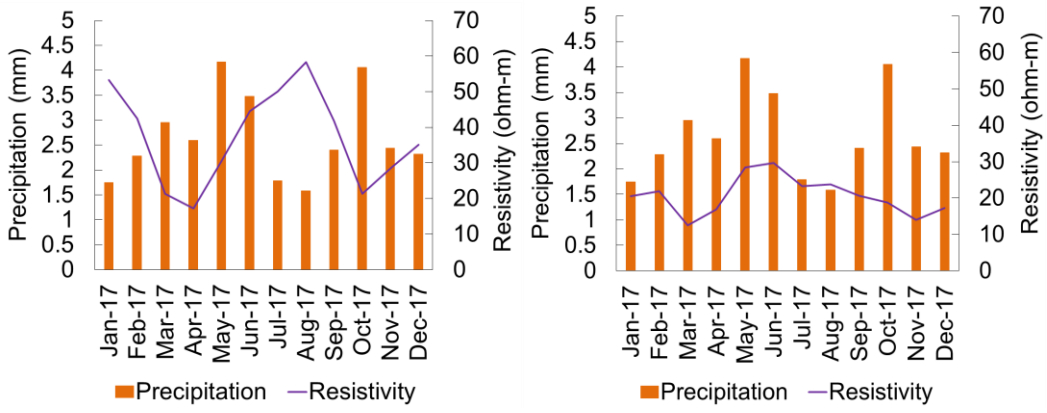

(a) (b)

Figure 4.15 Variation of mean resistivity with precipitation for Slope 1: (a) top 1.9 feet, (b) bottom 1.9 feet to 6 feet

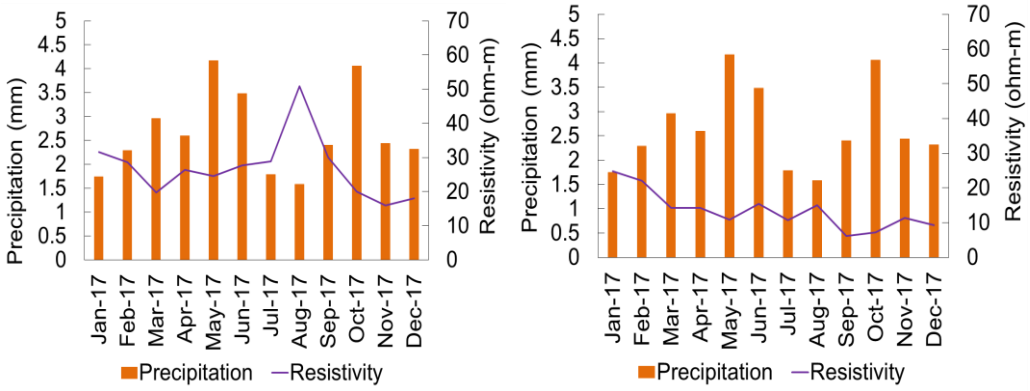

(a) (b)

Figure 4.16 Variation of mean resistivity with precipitation for Slope 2: (a) top 1.2 feet, (b) bottom 1.2 feet to 6 feet

Figure 4.17 and Figure 4.18 show the variation of resistivity with precipitation and depth. A remarkable relationship was found between the resistivity values along the soil transect and the precipitation. The resistivity values of Slope 1 and Slope 2 varied with the change of precipitation within the top 1.9 feet and 1.2 feet, respectively. In the top soil layer, there was an inverse relationship between soil resistivity and the amount of precipitation, but beneath the top soil layer, the relationship was weak.

Porosity is an indication of open space or voids in soil that are capable of retaining water (Easton, 2015). Pore space is the conduit that allows precipitated water to infiltrate and percolate the soil. Roots grow, following pathways of interconnected soil pores; primary root tips allow further opening of soil pores (Coder, 2000). During heavy precipitation, water can penetrate soil pores in the root zone. According to Kibria (2011), soil resistivity decreases with an increase of moisture content. Figure 4.17 and Figure 4.18 show that with an increase in precipitation, soil resistivity values decreased for both slopes within the top porous soil layer, confirming the presence of roots.

On the other hand, compaction reduces soil porosity (Pagliai, 1998). Infiltration rates are reduced significantly for compacted soils (Gregory et al., 2006; Pagliai, 1998). Beneath the root zone, the ET cover soil of the City of Irving Landfill is compacted and clayey. Due to the absence of roots, as well as pores, soil resistivity is primarily related to compacted soil properties. The compacted soil mass beneath the root zone of the ET cover does not allow water infiltration, and as a result, the soil resistivity beneath the root zone does not respond to the variations of precipitation. Figure 4.17 and Figure 4.18 show negligible changes in resistivity with precipitation beneath 1.9 feet and 1.2 feet depth for Slope 1 and Slope 2, respectively. This indicates an absence of roots in the above-mentioned layer of ET cover in the City of Irving Landfill.

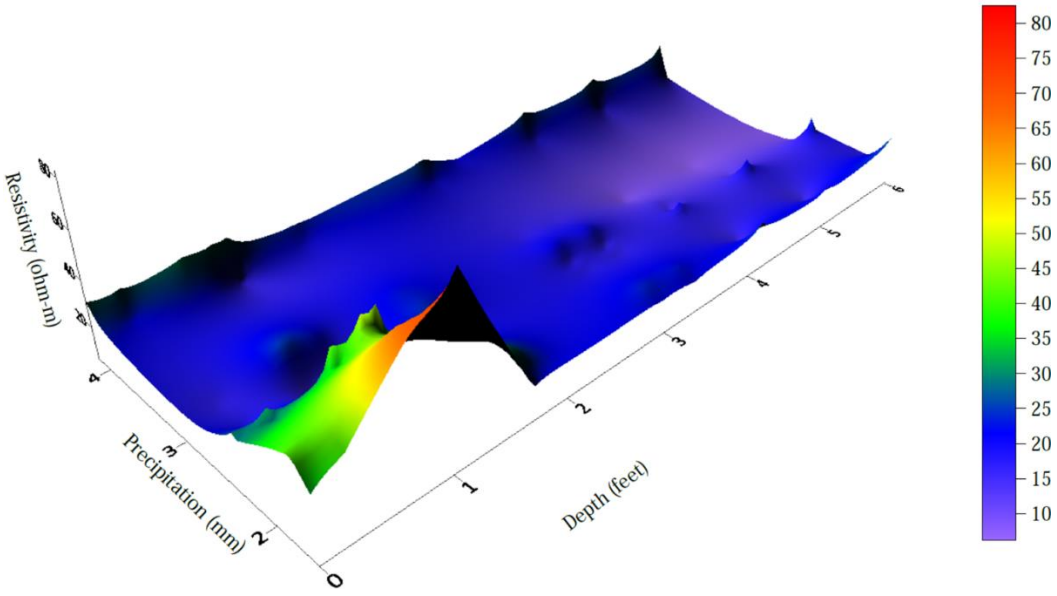

Figure 4.17 Three-dimensional surface area combining precipitation, depth, and resistivity for Slope 1

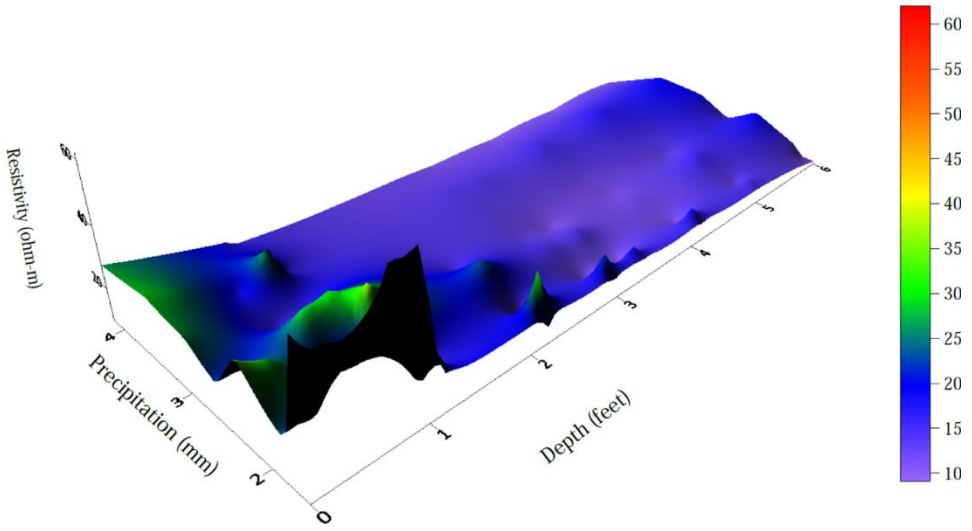

Figure 4.18 Three-dimensional surface area combining precipitation, depth, and resistivity for Slope 2

Variations in the resistivity with precipitation amount reconfirmed the effective rooting depth for both slopes, as depicted in Figure 4.19 and Figure 4.20. A good correlation was found between the mean resistivity of the root zone and the amount of precipitation; however, no satisfactory correlation was found between the mean resistivity of the non-root zone and precipitation.

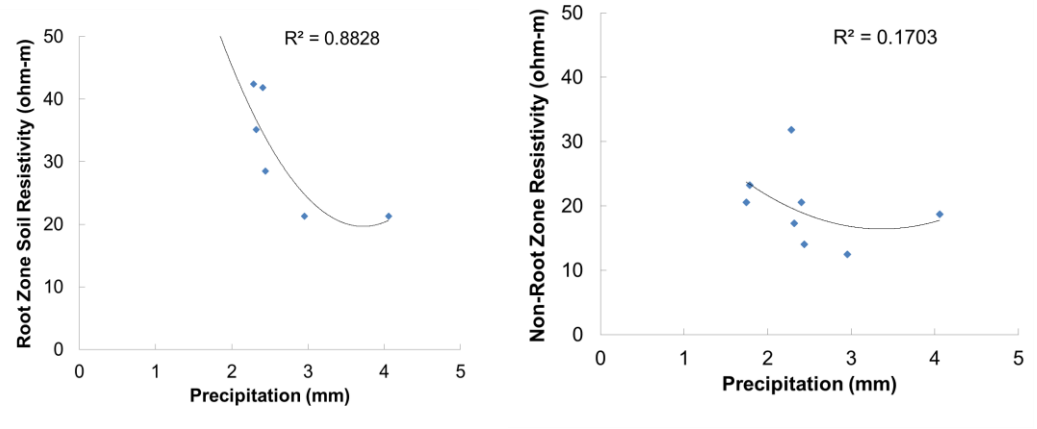

(a) (b)

Figure 4.19 Variation of soil resistivity with precipitation for Slope 1: (a) Root zone mean soil resistivity versus precipitation, (b) Non-root zone soil resistivity versus precipitation

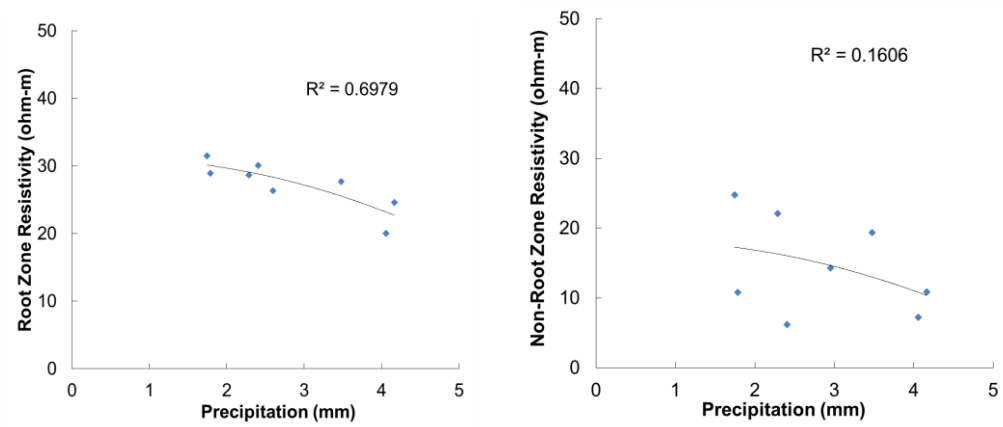

(a) (b)

Figure 4.20 Variation of soil resistivity with precipitation for Slope 1: (a) Root zone soil resistivity versus precipitation, (b) Non-root zone soil resistivity versus precipitation

4.4.3 Statistical Verification of ERI Data for Predicted Root Depth

Statistical analysis was done to identify the pattern of difference (both significant and non-significant) between the electrical resistivity values of estimated rooted and non-

rooted soil layers. A “t-test” analysis was performed to check whether the difference in resistivity between the two zones was significant. A t-test is an analysis of two sample means through the use of statistical examination. Statistical significance suggests that the two data set from which we sample are “actually” different.

For each season, the extracted electrical resistivity data from the full imaging profile was divided into two groups: root zone resistivity data and non-root zone resistivity data. The significance of difference between the two groups’ means was determined by the t-test analysis, which was run at 95% confidence interval, considering α=0.05. The alpha value was compared with the p-value for rejecting or accepting the null hypothesis. The P value, or calculated probability, is the probability of finding the observed, or more extreme, results when the null hypothesis is true. The null hypothesis in each case were considered that there was no difference between means of the two groups of data (mean of rooted layer soil resistivity and mean of non-rooted layer soil resistivity). When the p-value for the t-test is greater than α, the null hypothesis cannot be rejected. So if in this test, p-value comes as 0.85, where α=0.05, the null hypothesis cannot be rejected. However, if the p-value is 0.02, which is less than 0.05, the null hypothesis can be rejected. The rejection signifies that a significant difference exists between the means of the two groups of data. The results found from the t-test analysis are shown below in Table 4-5.

The t-test analysis showed that a significant difference existed between the rooted and non-rooted soil layers of both slopes in 2017, except during the winter. Growth patterns of roots are seasonal (Zornberg, Jorge G., et al., 2003 and Davidson, R. L., 1969). As the days shorten, from summer to winter, the progressive fall in soil temperature is greater than the fall in the air temperature, so that growth is limited mainly by the unfavorable edaphic environment (Davidson, R. L., 1969). According to Snyder, 2007, by all accounts, tree roots spend the winter in a condition of dormancy. They are not dead, but they overwinter in a

resting phase, with essential life processes continuing at a minimal rate. Full-on root growth resumes in spring, usually sometime before bud break. The dormancy of roots during winter explains the lack of significant difference between mean resistivity values in root zone and non-root zone soil layers. Thus, the t-test analysis shows a significant difference between the mean resistivity of rooted and non-rooted soil layers during the seasons when the root is actively transpiring. This implies that the presence of roots is responsible for the significant difference of resistivity between the root zone soil layer and non-root zone soil layer.

Table 4-5 Difference in resistivity between rooted and non-rooted zones of soil

Seasons	**Slope 1**		**Slope 2**	
	Remarks on difference in resistivity between rooted zone and non-rooted zone of soil (α=0.05)		**Remarks on difference in resistivity between rooted and non-rooted zone of soil (α=0.05)**	
	P value	Comment on difference	P value	Comment on difference
Winter	0.06230979	Difference not significant	0.0743402	Difference not significant
Spring	1.25472E-07	Significant difference	0.0015786	Significant difference
Early Summer	6.1483E-11	Significant difference	2.9125E-07	Significant difference
Late Summer	2.09931E-13	Significant difference	3.9162E-06	Significant difference
Early Fall	0.016580437	significant difference	1.649E-07	Significant difference
Late Fall	0.00087205	Significant difference	0.00441454	Significant difference

4.4.4 Verification of Predicted Root Depth Using Acrylic Tube (Minirhizotron)

An investigation of root length was performed based on the minirhizotron technique, with the root length being measured for both slopes. The minirhizotron technique offers two major advantages in the measurement of root depth: it minimizes destructive sampling, and the root growth can be observed (Alam, 2017). The image acquired from the minirhizotron was 4.5 inches wide and 3.0-inches high. Images taken during the monitoring period from inside the minirhizotron at a fixed interval of depth were

used to compute the root lengths of the two slopes. Results are presented for the two slopes at 0"-3" depth intervals. Each set is comprised of images up to the root being visible. The root length at the fixed depth of 0-3 inches is presented in Figure 4.21. Since, the length of each image was 3 inches, 7 images at 3 foot intervals represent the root length of 21 inches. Thus, the field investigation found that the root length for Slope 1 was 21 inches, or 1.75 feet; the root length for Slope 2 was 12 inches, or 1 foot (Figure 4.21).

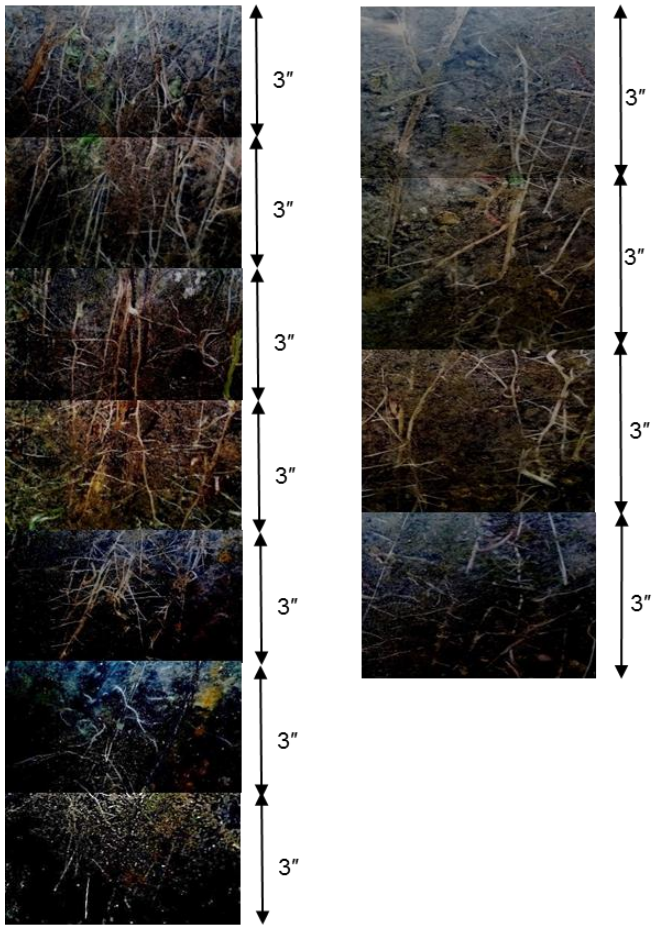

(a) (b)

Figure 4.21 Sections of root profile images at every 3-inch segment for (a) Slope 1 (b) Slope 2

4.4.5 Comparison of Field Investigation Results

Resistivity imaging was performed at the two slopes of the City of Irving Landfill to investigate the root length of the vegetation. At the same time, the roots were observed with the use of an acrylic tube to measure the actual root length. The length of roots found by analyzing the electrical resistivity data was compared with the actual root length found from the use of the acrylic tube, and the results are presented in Table 4-6.

Table 4-6 Comparison of field investigation results

Location of Slope	Field Investigation Method	Estimated Root length (feet)	Actual Root length (feet)	% difference
West Slope (Slope 1)	2D RI test	1.9	1.75	8.57
North Slope (Slope 2)	2D RI test	1.2	1	20

The comparison revealed very small differences in the predicted and actual root length, verifying that the electrical resistivity imaging technique is an effective tool for predicting the root length of vegetation in evapotranspiration cover soils.

4.4.6 Discussion of the Field Investigation Program

The RI test method was observed suitable for the determination of unknown root length of vegetation in ET cover soil. The 2D RI methods provided reasonably good results. The frequency plots of individual sections for high resistivity depths clearly marked the effective root length for the two slopes (Figure 4.10 and Figure 4.11). Distribution of resistivity data showed higher resistivity values and higher variations in the predicted rooted soil layer (Figure 4.12). The statistically significant difference between the means of the predicted rooted layer and non-rooted layer data signified the presence of roots in the high resistivity area (Table 4-5). The difference was not observed during the winter

because the roots were inactive under the frozen conditions of winter since they pass the winter in a prolonged dormancy marked by unbroken inactivity until spring (Snyder, 2007). The comparison of the predicted root length by resistivity imaging and the actual root length in the field showed only negligible differences, leading to the conclusion that the RI test was successful in determining the unknown root length of vegetation.

4.5 Analytical Modeling

Based on the variation of resistivity with precipitation and root length (Section 4.7.3), a multiple linear regression was performed, using the Minitab Student Version, to evaluate the root depth.

4.5.1 Data Collection

The vegetation in the slopes of City of Irving landfill was already developed at the time of investigation. For development of a model, it was necessary to know how much the resistivity varied with continuous root growth and regular changes in precipitation. Alam (2017) monitored vegetation growth and conducted experiments on six different lysimeters during 2015, 2016, and 2017 built beside each other in the City of Denton Landfill. For the current study, data from lysimeters 1, 2, 3, 4 and 6 was collected from Alam (2017) (Appendix A). Figure 4.22 and Figure 4.23 show schematics of the lysimeters.

Figure 4.22 Vegetative lysimeters (Alam, 2017)

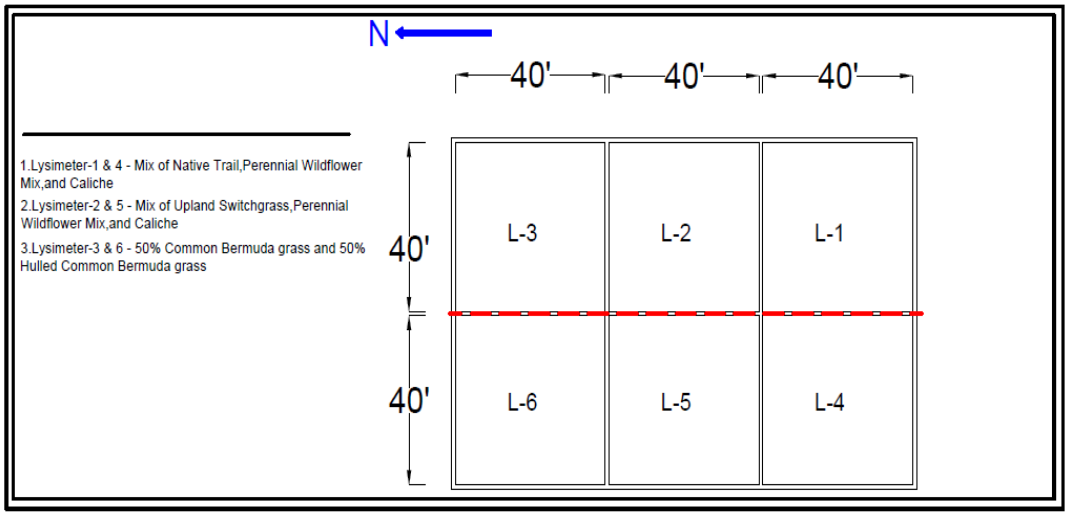

Figure 4.23 Detail of lysimeters (Alam, 2017)

Alam (2017) also performed electrical resistivity tests on the six lysimeters on a monthly basis. The physical arrangement allowed for direct comparison of different vegetative cover designs under the same climatic conditions with similar soil types. A complete weather station was installed at the site (City of Denton Landfill) to effectively monitor the meteorological data. Precipitation was continually monitored by the weather station, which has an automatic data recording system. Data for continuous root growth of vegetation (from seeding to final growth) in lysimeters 1, 2, 3, and 4 was taken simultaneously with data from the electrical resistivity testing and the recorded precipitation for development of analytical model (Appendix A).This data was applied to the current study.

4.5.2 Correlation Analysis

Correlation analysis helps in quantifying the liner association between two variables. The predictor variables in a multiple linear regression (MLR) model should not be correlated among themselves (Kutner et al., 2005). The primary concerns in determining

root length are raised from observing the variation of resistivity with precipitation and root length. Therefore, the predictor variables considered for the root depth model were:

- Mean resistivity of soil transect
- Precipitation

Since the unknown variable is root length, there is no way to separate the resistivity of rooted and non-rooted soil layers in a soil transect. So, the mean resistivity of the total soil transect was taken for model development.

Table 4-7 presents the Pearson's correlation coefficients computed for predictor vs. predictor. Pearson's correlation coefficient "r" ranges from -1 to +1, while -1 indicates a strong negative correlation and the +1 indicates a strong positive correlation between the parameters. When r=0, little or no correlation is indicated between the parameters.

Table 4-7 Pearson correlation coefficients

	Resistivity	**Precipitation**
Resistivity	1	-0.27535
Precipitation	-0.27535	1

From Table 4-7, it is seen that none of the r values were very high (r>0.7); however, the non-zero values indicated some correlations between the parameters. However, if r<0.7 it could be assumed, the multicollinearity would not be an issue for the data set.

4.5.3 Multiple Linear Regression (MLR) Equation

An attempt was made to develop a MLR model to evaluate root length, as follows:

$$R.L = \beta 1 \ + \ \beta 2 * R \ + \ \beta 3 * P$$

Where,

R.L = Root Length

R= Mean Resistivity of soil transect under consideration (ohm-m)

P = Precipitation (mm)

β1, β2, β3 = correlation parameters were determined from multiple linear regression. After performing linear regression, using the data (collected from Alam, 2017), the above equation took the form of

$$Root\ length = 0.2906 + 0.02155\ Resistivity + 0.01537\ Precipitation \ldots\ldots\ldots\ldots\ldots\ldots (4.1)$$

A coefficient of determination (adjusted R^2=70.83) adequate for a field-level investigation was found. Figure 4.24 shows the regression modeling output between mean resistivity of soil transect, precipitation, and root length. Standardized residual plot, normal probability plot, histogram, and the order plot are also given separately in Figure 4.25.

Regression Analysis: Root length versus Resistivity, Precipitation

Analysis of Variance

Source	DF	Adj SS	Adj MS	F-Value	P-Value
Regression	2	6.2817	3.14084	116.36	0.000
Resistivity	1	6.1848	6.18481	229.13	0.000
Precipitation	1	0.1487	0.14866	5.51	0.021
Error	93	2.5103	0.02699		
Total	95	8.7920			

Model Summary

S	R-sq	R-sq(adj)	R-sq(pred)
0.164294	71.45%	70.83%	69.67%

Coefficients

Term	Coef	SE Coef	T-Value	P-Value	VIF
Constant	0.2906	0.0555	5.24	0.000	
Resistivity	0.02155	0.00142	15.14	0.000	1.08
Precipitation	0.01537	0.00655	2.35	0.021	1.08

Regression Equation

Root length = 0.2906 + 0.02155 Resistivity + 0.01537 Precipitation

Fits and Diagnostics for Unusual Observations

Obs	Root length	Fit	Resid	Std Resid	
46	1.1667	0.8222	0.3445	2.12	R
68	1.5000	1.1474	0.3526	2.16	R
69	1.5000	1.1508	0.3492	2.14	R
77	0.5000	0.8270	-0.3270	-2.08	R

R Large residual

Figure 4.24 Model output

Figure 4.25 Normal probability plot, residual plot, histogram, and order plot of the linear regression between resistivity, precipitation, and root length

The histogram (Figure 4.25) shows that the model is multimodal, which is an indication of several patterns of response or extreme views of the sample. It also depicts the preferences or attitudes of the sample which yielded the necessity for variable transformation.

Log-function was considered for the transformation of root length. After applying the logarithmic function on the response side, the equation takes the following form:

$$ln(Root\ length) = -0.9091 + 0.02574\ Resistivity + 0.02070\ Precipitation \quad \text{.....(4.2)}$$

A good trend with symmetric distribution of residuals was observed when the root length was transformed. From Figure 4.26, it is seen that the normal probability plot

followed the straight line pattern, indicating the Gaussian distribution of data points around the mean, which is also supported by the bell-shaped histogram. There was a negligible change in the coefficient of determination (adjusted R^2=68.30) shown in Figure 4.27.

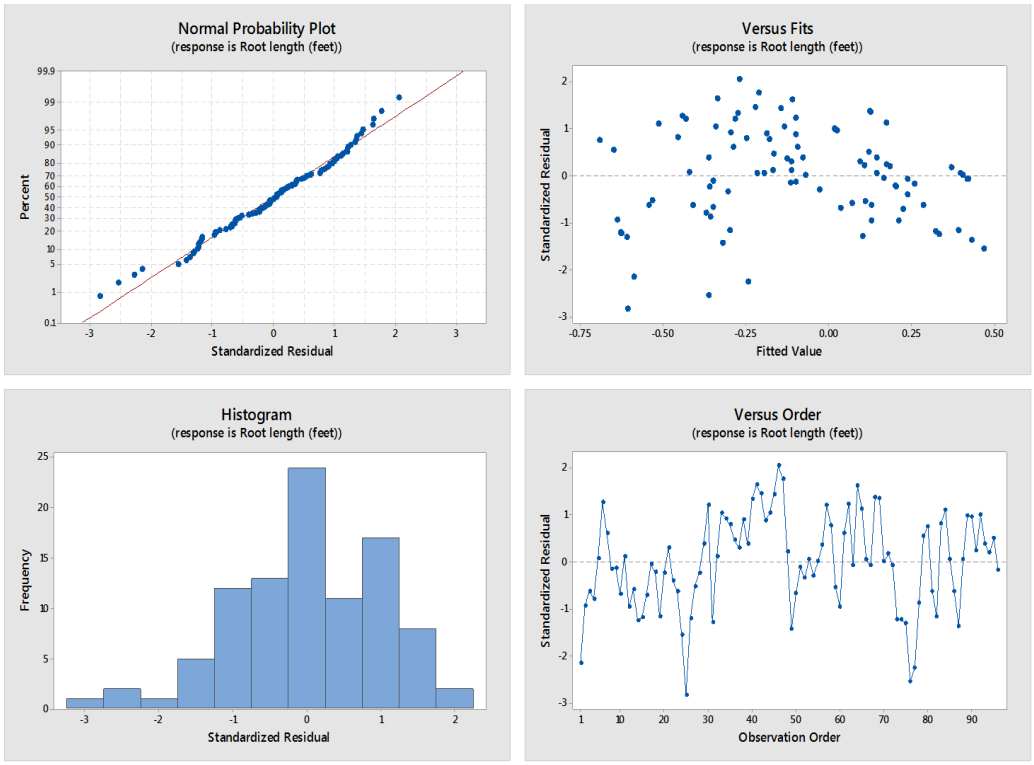

Figure 4.26 Normal probability plot, residual plot, histogram, and order plot of the linear regression between resistivity, precipitation, and root length

Both the intercept and the variable coefficient of the model were found to be significant in terms of P-values. In Minitab, the null hypothesis is that there is no interaction between the two independent variables (resistivity and precipitation) on the dependent variable (root length). From the P-values it is seen that the interaction effect is statistically significant (P value= 0.00 for regression model). A statistically significant interaction means that the effect of the root length is dependent on resistivity (and vice versa); that is, the effect of resistivity on root length is dependent on precipitation. The residuals-versus-fits

plot shows that the residuals were randomly distributed with no recognizable patterns in the points, meaning that the residuals were consistent, with random error. In the order plot, residuals exhibiting normal random noise around the residual = 0 line suggest that there was no serial correlation.

Regression Analysis: Root length versus Resistivity, Precipitation

Method

Box-Cox transformation λ = 0

Analysis of Variance for Transformed Response

Source	DF	Adj SS	Adj MS	F-Value	P-Value
Regression	2	8.9250	4.46251	103.36	0.000
Resistivity	1	8.8284	8.82840	204.49	0.000
Precipitation	1	0.2697	0.26968	6.25	0.014
Error	93	4.0151	0.04317		
Total	95	12.9401			

Model Summary for Transformed Response

S	R-sq	R-sq(adj)	R-sq(pred)
0.207781	68.97%	68.30%	66.79%

Coefficients for Transformed Response

Term	Coef	SE Coef	T-Value	P-Value	VIF
Constant	-0.9091	0.0701	-12.96	0.000	
Resistivity	0.02574	0.00180	14.30	0.000	1.08
Precipitation	0.02070	0.00828	2.50	0.014	1.08

Regression Equation

ln(Root length) = -0.9091 + 0.02574 Resistivity + 0.02070 Precipitation

Fits and Diagnostics for Unusual Observations

Original Response

Obs	Root length	Fit
1	0.3583	0.5552
25	0.3067	0.5457
46	1.1667	0.7646
76	0.4167	0.6968
77	0.5000	0.7848

Fits and Diagnostics for Unusual Observations

Transformed Response

Obs	Root length'	Fit	Resid	Std Resid	
1	-1.0263	-0.5884	-0.4379	-2.15	R
25	-1.1820	-0.6058	-0.5762	-2.84	R
46	0.1542	-0.2684	0.4225	2.05	R
76	-0.8755	-0.3612	-0.5143	-2.54	R
77	-0.6931	-0.2423	-0.4508	-2.27	R

Root length' = transformed response
R Large residual

Figure 4.27 Model output

4.5.4 Model Verification

The data of lysimeter 6 from the City of Denton Landfill was used to verify the regression model. Alam (2017) observed the continuous root growth of vegetation in lysimeter 6 for the years 2015, 2016, and 2017. Figure 4.28 shows the comparison between the predicted root length from the proposed model and the actual root length observed by Alam (2017), and shows that the predicted values were within 3-9% of the actual values. Figure 4.29 and Figure 4.30 show the comparison between the predicted root length from the proposed model and actual root length observed with the minihizotron in the ET cover of Slope 1 and Slope 2 of the City of Irving Landfill. Predicted values for Slope 1 of the City of Irving Landfill were within 5-10% of the actual values of root length of vegetation. Predicted values for Slope 2 of the landfill varied up to 13% of the actual values of the root length. Table 4-8 shows the percent of difference between the actual and predicted root lengths for different site locations.

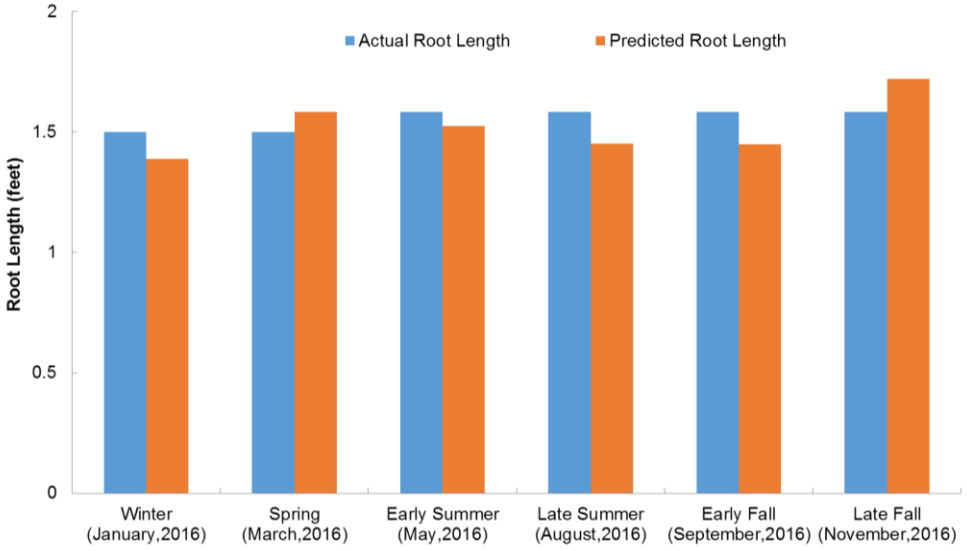

Figure 4.28 Comparison between predicted and actual root length of ET cover of City of Denton Landfill

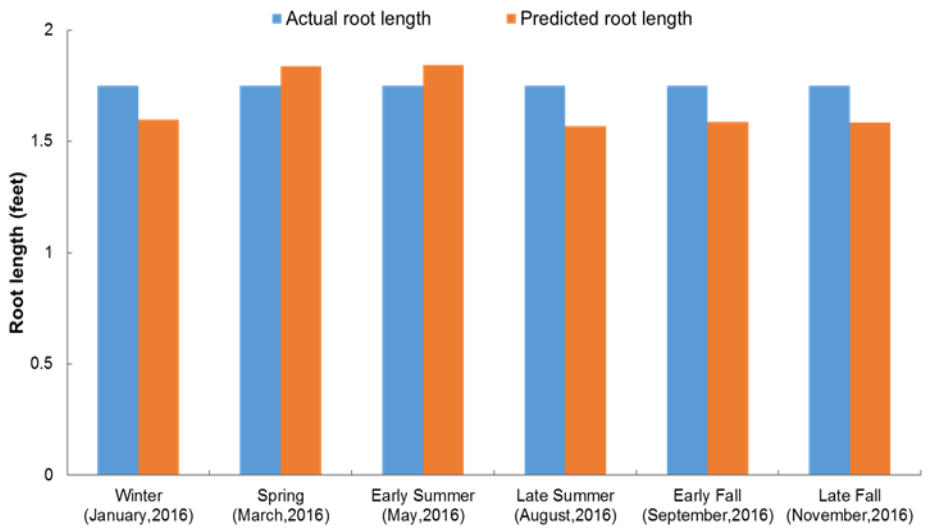

Figure 4.29 Comparison between predicted and actual root length of ET cover of Slope 1 of City of Irving Landfill

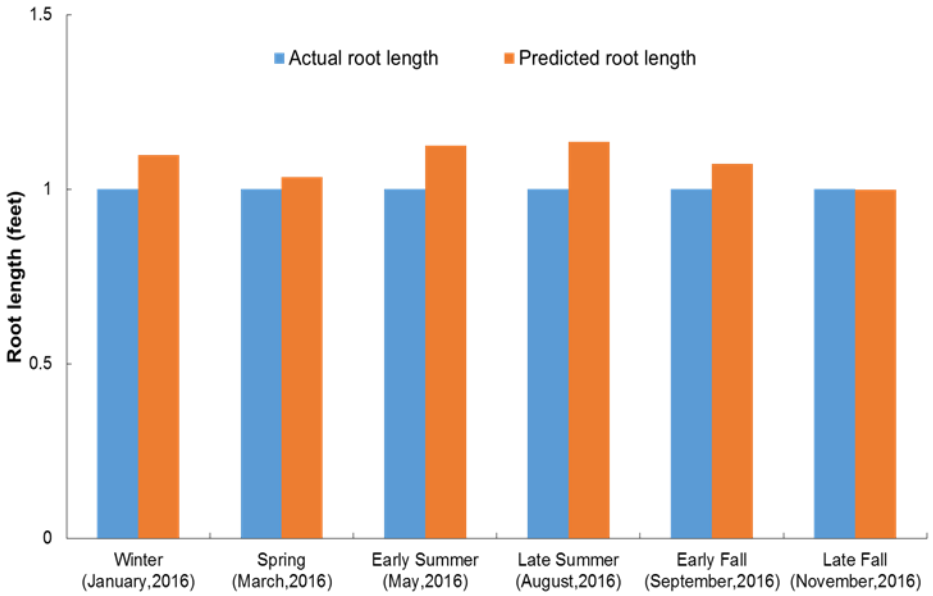

Figure 4.30 Comparison between predicted and actual root length of ET cover of Slope 2 of City of Irving Landfill

Table 4-8 Percent variation of predicted and actual values

	Percent variation between actual and predicted root length					
Site Location	Winter (January, 2016	Spring (March, 2016)	Early Summer (May, 2016)	Late Summer (August, 2016)	Early Fall (September, 2016)	Late Fall (November, 2016)
Lysimeter 6 (City of Denton Landfill)	7.47	5.58	3.63	8.32	8.42	8.59
Slope 1 (City of Irving Landfill)	8.70	5.01	5.38	10.41	9.24	9.42
Slope 2 (City of Irving Landfill)	9.87	3.51	12.59	13.50	7.36	0.18

Figure 4.31 represents the comparison between the actual root lengths with the predicted values for all sites. The trends show that the variation of predicted values fell within the bands of a15% error margin, indicating good agreement between the actual and predicted values.

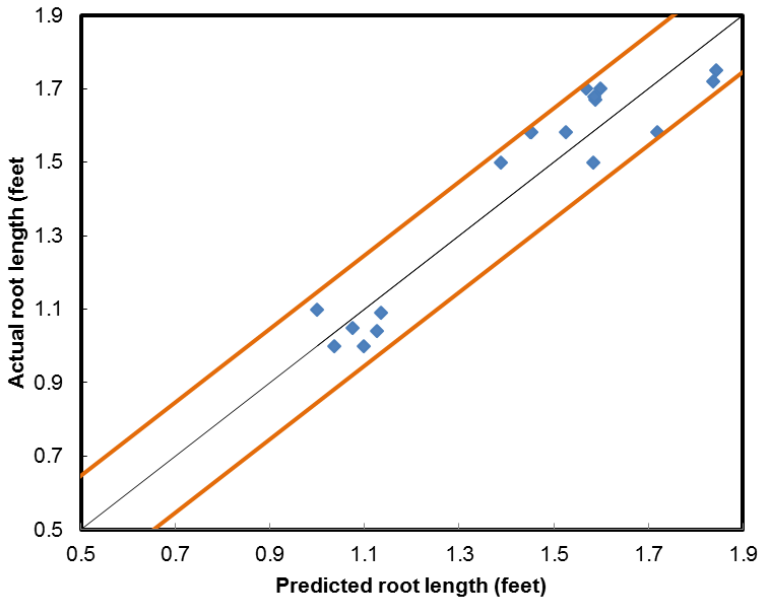

Figure 4.31 Comparison between the actual root lengths with the predicted root lengths

4.5.5 Limitations

The current study assumed a mean resistivity of total soil transect for a particular day of the month and considered the average precipitation for the month. However, values of soil electrical resistivity varied every single day with variations in precipitation. Data from the National Weather Service and Weather Underground indicates that cities in North Central Texas experience the most unpredictable weather (Nate Silver and Reuben Fischer-Baum, 2014). The list was compiled by examining weather that deviates from long-term patterns, with an eye on temperature, precipitation, and severe weather conditions. This signifies that day-to-day changes of resistivity with day-to-day changes of temperature and precipitation adds values to the precision of the model.

Detail of soil properties did not get concentration while modeling, which may be another reason for of variations from the actual result. Parameters describing soil properties can be added to the model to increase accuracy and versatility.

Absorption by roots is largely a function of soil temperature, moisture tension, nutrient concentration, and soil oxygen (Davidson, R. L., 1969). Since the interacting edaphic factors determine root activity, adding these factors to the modeling could add precision to the model.

Chapter 5

CONCLUSION

The effect of plant root growth is tremendously important in determining the performance of ET cover. The objective of this study was to evaluate electrical resistivity as a non-destructive method to determine root length. The current study presents the determination of unknown root length, using electrical resistivity imaging, at two final covers at the City of Irving landfill. The study also aimed at developing an analytical model for determination of root length, using soil resistivity values and precipitation amounts.

5.1 Summary and Conclusions

The investigation results can be summarized as:

- 2D resistivity imaging was performed at Slope 1 and Slope 2 of the ET cover at the City of Irving landfill to determine the root length of vegetation. A high resistivity zone was found from the distribution of resistivity, which was estimated as root length. The root length estimated from RI was 1.9 feet for Slope 1 and 1.2 feet for Slope 2.
- Good correlation was found between the mean resistivity of the estimated root zone and the amount of precipitation. Weak correlation was found between the mean resistivity of the estimated non-root zone and the amount of precipitation.
- A statistically significant difference was found between the resistivity values of the predicted root zone soil layer and the non-root zone soil layer in all seasons, except in winter, when the roots were dormant.
- Root length was investigated in the field based on the minirhizotron technique. The actual root lengths for Slope 1 and Slope 2 were 1.75 feet and 1 foot, respectively.
- The resistivity imaging was effective at determining the length of roots in evapotranspiration cover soil.

- A multiple linear regression model was developed to evaluate root length. The mean resistivity of the soil transect and amount of precipitation were selected as two independent variables for determination of root length. The model is presented in Equation 4.1.
- The MLR assumptions were not satisfied in the preliminary model. Thus, the root length was transformed to ln(root length) to improve the model. The finalized model form for determining root length can be described as:

$$\ln(Root\ length) = -0.9091 + 0.02574\ Resistivity + 0.02070\ Precipitation$$

Here, root length is in feet, mean resistivity of transect is in ohm-m, and precipitation is in mm.

5.2 Recommendation for Future Studies

To make the current study even more effective, it is recommended that the work be continued, as follows:

- The current study assumed average resistivity and average precipitation per day for a particular month. However values of electrical resistivity vary every single day with variations of precipitation. A future study could incorporate values of continuous electrical resistivity tests per day with variations of precipitation.
- As this study focused only on compacted landfill cover soil, a future study could be conducted to determine the effects of different levels of soil compaction on root length of vegetation.
- A versatile range of vegetation and soil type properties could be incorporated in future modeling with a view to evaluating root length by non-destructive electrical resistivity imaging test.

Appendix A

Data Set for Analytical Modeling

Table 1 Data from City of Denton Landfill (Alam, 2017)

Resistivity (ohm-m)	Precipitation (mm/day)	Root length (feet)
10.53956481	2.384322581	0.358333333
7.840654762	3.311071429	0.435416667
12.52462281	2.163096774	0.5125
13.82464657	8.881533333	0.589583333
10.03825	11.07767742	0.666666667
15.30146065	3.5306	0.833333333
23.2230625	1.188064516	0.849673203
30.75775926	0.155677419	0.866013072
29.5646713	2.370666667	0.882352941
32.4133	5.28483871	0.89869281
24.03825	8.619066667	0.916666667
37.30146065	3.81	0.933006536
37.57293452	0.598129032	0.949346405
46.82063382	1.813034483	1.083333333
44.54714833	4.039419355	1.083333333
39.29272826	5.952066667	1.083333333
36.57529545	6.415548387	1.166666667
39.50488958	4.445	1.166666667
48.32495	2.785806452	1.166666667
39.9661375	3.998451613	1.166666667
36.14501042	3.4798	1.166666667
42.58252083	2.384322581	1.166666667
43.28873958	3.8354	1.166666667
52.93563021	0.688258065	1.166666667
9.86453473	2.384322581	0.306666667
8.23657495	3.311071429	0.4175
12.91079868	2.163096774	0.528333333
14.2509065	8.881533333	0.666666667
12.3485	11.07767742	0.75
15.7738	3.5306	0.833333333
38.33819	1.188064516	0.849673203
28.64245	0.155677419	0.866013072
20.16791533	2.370666667	0.882352941
19.5334	5.28483871	0.89869281
18.7904	8.619066667	0.916666667
25.83492235	3.81	0.933006536
30.4231	0.598129032	0.949346405

Resistivity (ohm-m)	Precipitation (mm/day)	Root length (feet)
26.5859367	1.813034483	1
29.05735207	4.039419355	1
19.88758738	5.952066667	1
17.08636706	6.415548387	1
23.13712	4.445	1.083333333
29.19830263	2.785806452	1.083333333
26.89009	3.998451613	1.083333333
26.95114824	3.4798	1.166666667
22.97048189	2.384322581	1.166666667
24.00680905	3.8354	1.166666667
38.95115	0.688258065	1.166666667
20.9558	2.384322581	0.540833333
19.1429	3.311071429	0.613958333
19.9805	2.163096774	0.687083333
16.3387	8.881533333	0.687083333
18.88317	11.07767742	0.833333333
31.4426	3.5306	0.916666667
31.64245	1.188064516	0.933006536
30.3249	0.155677419	0.949346405
22.4099	2.370666667	0.965686275
24.1032	5.28483871	0.982026144
32.6778	8.619066667	1
40.49585	3.81	1.016339869
31.21133168	0.598129032	1.032679739
30.02321914	1.813034483	1.166666667
41.25404167	4.039419355	1.25
26.23268667	5.952066667	1.25
36.93229167	6.415548387	1.5
47.11989484	4.445	1.5
49.43993827	2.785806452	1.5
36.90909211	3.998451613	1.5
37.43993827	3.4798	1.5
49.07078704	2.384322581	1.5
46.63948438	3.8354	1.5
51.01807407	0.688258065	1.5
9.017	2.384322581	0.416666667
8.388	3.311071429	0.416666667
9.932	2.163096774	0.416666667

Resistivity (ohm-m)	Precipitation (mm/day)	Root length (feet)
14.14	8.881533333	0.416666667
16.991	11.07767742	0.5
18.629	3.5306	0.583333333
9.142	1.188064516	0.583333333
8.323	0.155677419	0.583333333
17.47	2.370666667	0.583333333
19.503	5.28483871	0.583333333
10.721	8.619066667	0.75
12.271	3.81	0.75
26.427	0.598129032	0.815359477
38.909	1.813034483	1
48.869	4.039419355	1.166666667
36.117	5.952066667	1.166666667
30.942	6.415548387	1.25
32.712	4.445	1.25
39.792	2.785806452	1.25
32.796	3.998451613	1.25
38.101	3.4798	1.25
40.538	2.384322581	1.25
36.913	3.8354	1.25
44.832	0.688258065	1.25

References

1. Ahmed, A., Hossain, M. S., Khan, M. S., Greenwood, K., and Shishani, A. (2017, July). Moisture Variation in Expansive Subgrade Through Field Instrumentation and Geophysical Testing. In International Congress and Exhibition" Sustainable Civil Infrastructures: Innovative Infrastructure Geotechnology"(pp. 45-58). Springer, Cham.
2. Ahmed, A., Hossain, M.S., and Khan, M.S. (2018). Monitoring of Moisture Variation in Highway Slope through Resistivity Imaging. Proceedings of International Foundation Congress and Equipment Expo, IFCEE, Orlando, FL.
3. Alam, M. J. B. (2017) "Evaluation of Plant Root on the Performance of Evapotranspiration (ET) Cover System". Ph.D. Dissertation, University of Texas at Arlington, October 2017.
4. Albright, W. and Benson, C. (2005). “Alternative cover assessment program: Report to Office of Research and Development National Risk Management Research Lab Land Remediation and Pollution Control Division. Desert Research Institute and University of Wisconsin, 54 pp.
5. Albright, W. H.; Benson, C. H.; and Waugh, W. J. (2010). “Water balance covers for waste containment: Principles and practice.” American Society of Civil Engineers.
6. Albright, William H., et al. (2004). "Field water balance of landfill final covers." Journal of Environmental Quality, vol. 33.6, pp. 2317-2332.
7. Amato, M., Basso, B., Celano, G., Bitella, G., Morelli, G., & Rossi, R. (2008). In situ detection of tree root distribution and biomass by multi-electrode resistivity imaging. *Tree physiology*, *28*(10), 1441-1448.
8. Attia al Hagrey, S. (2007). Geophysical imaging of root-zone, trunk, and moisture heterogeneity. *Journal of Experimental Botany*, *58*(4), 839-854.

9. Barnett, D. P.; Paul, J. L.; Harris, R. W.; & Henderson, D. W. (1983). “Estimating root length densities around transplanted container-grown plants.” Journal of Arboriculture (USA).
10. Barnswell, K. D., & Dwyer, D. F. (2010). “Assessing the performance of evapotranspiration covers for municipal solid waste landfills in Northwestern Ohio.” Journal of Environmental Engineering, vol. 137(4), pp. 301-305.
11. Benson, C. and Bareither, C. (2012). “Designing water balance covers for sustainable waste containment: Transitioning state of the art to state of the practice. Geotechnical Engineering State of the Art and Practice: pp. 1-33.
12. Benson, C. H.; Albright, W. H.; Roesler, A. C.; & Abichou, T. (2002). “Evaluation of final cover performance: field data from the alternative cover assessment program (ACAP).” Proc. Waste Management, vol. 2, pp. 1-15.
13. Benson, C.H. et al. (2002). “Evaluation of final cover performance: Field data from the Alternative Landfill Cover Assessment Program (ACAP).” Proceedings, WM 2002 Conference. Tucson, Arizona. February 24-28.
14. Böhm, W. (1979). *“Container methods.”* In Methods of studying root systems (pp.. 95-114). Springer Berlin Heidelberg.
15. Bonaparte, R.; Daniel, D.; and Koerner, R. M. (2002). “Assessment and recommendations for improving the performance of waste containment systems.” EPA-Environmental Protection Agency, p. 1039.
16. Coder, K. D. (2000). “Soil compaction & trees: Causes, symptoms & effects.” University of Georgia School of Forest Resources, Athens, GA. pp. 1-37.
17. Dannoura, M.; Kominami, Y.; Oguma, H.; & Kanazawa, Y. (2008). “The development of an optical scanner method for observation of plant root dynamics.” Plant Root, vol. 2, pp. 14-18.

18. Davidson, R. L. (1969) "Effect of root/leaf temperature differentials on root/shoot ratios in some pasture grasses and clover." Annals of Botany, vol. 33.3, pp. 561-569.
19. Dwyer, S.F.; Stormont, J.C.; and Anderson, C.E. (1999). “Mixed waste landfll design report.” Sandia National Laboratories. SAND99-2514. October.
20. Dwyer, Stephen F. (2003). “Water balance measurements and computer simulations of landfill covers.” Dissertation, University of New Mexico.
21. Easton, Zachary M., and Emily Bock (2015). "Hydrology basics and the hydrologic cycle."
22. Fort, F., Volaire, F., Guilioni, L., Barkaoui, K., Navas, M. L., & Roumet, C. (2017). Root traits are related to plant water-use among rangeland Mediterranean species. *Functional Ecology*.
23. Glinski, D. S.; Karnok, K. J.; and Carrow, R. N. (1993). “Comparison of reporting methods for root growth data from transparent-interface measurements.” Crop Science, vol. 33(2), pp. 310-314.
24. Goldenberg, M., & Reddy, K. R. (2012). “Sustainability assessment of conventional and alternate landfill cover systems.” In Geotechnical Frontiers 2017 (pp.. 323-332).
25. Gregory, Justin H., et al. (2006). "Effect of urban soil compaction on infiltration rate." Journal of soil and water conservation, vol. 61.3, pp. 117-124.
26. Hakonson, T. E.; Karr, L.; & Harre, B. (1997). “A water balance study of infiltration control landfill cover designs at Marine Corp Base, Hawaii. In landfill capping in the semi-arid west: Problems, perspectives, and solutions. Proceedings of the Environmental Science and Research Foundation Conference.
27. Hauser, V. L. (2009). Evapotranspiration covers for landfills and waste sites. Resource, Engineering & Technology for a Sustainable World, 16(3), 14-15.

28. Hauser, Victor L.; Weand, Barron L.; and Gill, Marc D. (2001) "Natural covers for landfills and buried waste." Journal of Environmental Engineering, vol. 127.9, pp. 768-775.
29. Hossain, M. I. (2017) "Non-destructive Evaluation of Soil Moisture in Evapotranspiration Cover System". Ph.D. Dissertation, University of Texas at Arlington, November 2017.
30. Silver, N. and Fischer-Baum, R. (2014). "Which City Has The Most Unpredictable Weather?" <*https://fivethirtyeight.com/features/which-city-has-the-most-unpredictable-weather/* > *(December 4, 2014)*
31. Huck, M. G., & Taylor, H. M. (1982). "The rhizotron as a tool for root research." Advances in agronomy, vol. 35, pp. 1-35.
32. Ingram, K. T., & Leers, G. A. (2001). "Software for measuring root characters from digital images." Agronomy Journal, vol. 93(4), pp. 918-922.
33. Ingram, K. T., & Leers, G. A. (2001). "Software for measuring root characters from digital images." Agronomy Journal, 93(4), 918-922.
34. ITRC. 2003b. "Technical and regulatory guidance for design, installation, and monitoring of alternative final landfill covers." 198 pp.
35. Jayawickreme, Dushmantha H.; Van Dam, Remke L.; and Hyndman, David W. (2008). "Subsurface imaging of vegetation, climate, and root-zone moisture interactions." Geophysical Research Letters, vol. 35.18.
36. Jones, C. A. (1983). "Effect of soil texture on critical bulk densities for root growth." Soil Science Society of America Journal, vol. 47(6), pp. 1208-1211.
37. Kano-Nakata, M.; Inukai, Y.; Wade, L. J.; Siopongco, J. D. C.; and Yamauchi, A. (2011). "Root development, water uptake, and shoot dry matter production under water

deficit conditions in two CSSLs of rice: Functional roles of root plasticity." Plant Production Science, vol. 14(4), pp. 307-317.

38. Kearey, P.; Brooks, M.; and Hill, I. (2002). *"An introduction to geophysical exploration."*
39. Khan, M. S. (2011). Evaluation of Resistivity Imaging (RI) Method for Determining Unknown Deep Foundation Depth..
40. Khire, Milind V.; Craig H. Benson; and Peter J. Bosscher (1997), "Water balance modeling of earthen final covers." Journal of Geotechnical and Geoenvironmental Engineering, vol. 123.8, 744-754.
41. Kibria, G. (2014). *Evaluation of physico-mechanical properties of clayey soils using electrical resistivity imaging technique*. The University of Texas at Arlington.
42. Klepper, B., & Kaspar, T. C. (1994). "Rhizotrons: Their development and use in agricultural research." Agronomy Journal, vol. 86(5), pp. 745-753.
43. Koerner, R. M., & Daniel, D. E. (1997). Final covers for solid waste landfills and abandoned dumps. Thomas Telford.
44. Kono, Y.; Yamauchi, A.; Nonoyama, T.; Tatsumi, J.; and Kawamura, N. (1987). "A revised experimental system of root-soil." Interaction for Laboratory Work. Environment Control in Biology, vol. 25(4), pp. 141-151.
45. Lazzari, L. (2008). "Study of spatial variability of soil root zone proper ties using electrical resistivity technique." Ph.D. Dissertation, University of Basilicata, Potenza, Italy, 107 p
46. Loke, M. H. (1999). Electrical imaging surveys for environmental and engineering studies. *A practical guide to*, *2*.
47. Maganti, D. (2009). "Subsurface investigations using high resolution resistivity." MS Thesis, UT Arlington, Arlington, TX.

48. Malusis, M. A. and Benson, C. H. (2006). “Lysimeter versus water-content sensors for performance monitoring of alternative earthen final covers.” Unsaturated Soils, pp.. 741-752.
49. McBean, E.A.; Roves, F.A.; Farquhar, G.J. (1995). *“Solid waste landfill engineering and design.” Prentice Hall PTR, Englewood Cliffs, NJ.*
50. McDougall, W. B. (1916). "The growth of forest tree roots." American Journal of Botany, vol. 3.7, pp. 384-392.
51. Morelli, G.; Zenone, T.; Teobaldelli, M.; Fischanger, F.; Matteucci, M.; & Seufert, G. (2007). “Use of ground-penetrating radar (GPR) and electrical resistivity tomography (ERT) to study tree roots volume in pine forest and poplar plantation.” Napier, New Zealand, vol. 21, pp. 1-4.
52. Pagliai, M. (1998). "Changes of pore system following soil compaction." Experiences with the impact and prevention of subsoil compaction in the European Community.
53. Paglis, Carlos Mauricio (2013) "Application of electrical resistivity tomography for detecting root biomass in coffee trees." International Journal of Geophysics 2013.
54. Panissod, C.; Michot, D.; Benderitter, Y.; and Tabbagh, A. (2001). “On the effectiveness of 2D electrical inversion results: An agricultural case study.” Geophysical Prospecting, vol. 49(5), pp. 570-576.
55. Patena, G., & Ingram, K. T. (2000). “Digital acquisition and measurement of peanut root minirhizotron images.” Agronomy Journal, vol. 92(3), pp. 541-544.
56. Rock, S. A. (2010). "Evapotranspiration covers for landfills." *Application of Phytotechnologies for Cleanup of Industrial, Agricultural, and Wastewater Contamination*. Springer, Dordrecht, pp. 189-198.
57. Rock, S.; Myers, B.; and Fiedler, L. (2012). “Evapotranspiration (ET) covers.” International Journal of Phytoremediation, vol. 14(S1), pp. 1-25.

58. Schuurman, J. J. (1971). "Effect of supplemental fertilization on growth of oats with restricted root development." Z Acker--and Pflanz.
59. Smit, A. L.; George, E., and Groenwold, J. (2000) *"Root observations and measurements at (transparent) interfaces with soil."* Root Methods. Springer, Berlin, Heidelberg, pp. 235-271.
60. Snyder, M. (2007). "What Do Tree Roots Do in Winter?" <*https://northernwoodlands.org/articles/article/what_do_tree_roots_do_in_winter* > (December 1, 2007)
61. Stormont, J. and Morris, C. (1998). "Method to estimate water storage capacity of capillary barriers." J. Geotech. Geoenviron. Eng., vol. 124(4), pp. 297-302.
62. Stormont, John C. (1997) "Incorporating capillary barriers in surface cover systems." Landfill Capping in the Semi-Arid West: Problems, Perspectives, and Solutions, Conference Proceedings, ESRF-019, Environmental Science and Research Foundation.
63. Sun, S. J., Meng, P., Zhang, J. S., & Wan, X. (2011). Variation in soil water uptake and its effect on plant water status in Juglans regia L. during dry and wet seasons. Tree physiology, 31(12), 1378-1389.
64. Tabbagh, A.; Dabas, M.; Hesse, A.; & Panissod, C. (2000). "Soil resistivity: a non-invasive tool to map soil structure horizonation." Geoderma, vol. 97(3), pp. 393-404.
65. Tabbagh, J., Samouëlian, A., Tabbagh, A., & Cousin, I. (2007). Numerical modelling of direct current electrical resistivity for the characterisation of cracks in soils. *Journal of Applied Geophysics*, *62*(4), 313-323.
66. Taylor, H.M.; Upchurch, D.R.; and McMicheal, B.L. (1990). "Applications and limitations of rhizotrons and minirhizotrons for root studies." Plant and Soil, vol. 129, pp. 29-35.

67. Van Noordwijk, M., et al. (1991). "Plant roots and their environment." Plant roots and their environment.
68. Vegapareddy, M.; Richter, G.M., and Goulding, K. W. T. (2010). "Using digital image analysis to quantify the architectural parameters of roots grown in thin rhizotrons." Plant Biosystems, vol. 144.2, pp. 499-506.
69. Weaver, J. E.; Jean, F. C.; & Crist, J. W. (1922). “Development and activities of roots of crop plants: A study in crop ecology (No. 316).” Carnegie Institution of Washington.
70. Zenone, T.; Morelli, G.; Teobaldelli, M.; Fischanger, F.; Matteucci, M.; Sordini, M.; and Seufert, G. (2008). “Preliminary use of ground-penetrating radar and electrical resistivity tomography to study tree roots in pine forests and poplar plantations.” Functional Plant Biology, vol. 35(10), pp. 1047-1058.
71. Zornberg, Jorge G.; LaFountain, Lester; and Caldwell, Jack A. (2003). "Analysis and design of evapotranspirative cover for hazardous waste landfill." Journal of Geotechnical and Geoenvironmental Engineering, vol. 129.5, pp. 427-438.

Biographical Information

Fouzia Hossain Oyshi graduated with a Bachelor of Science in Civil Engineering from Bangladesh University of Engineering and Technology, Dhaka, Bangladesh in March, 2016. She started her graduate studies at the University of Texas at Arlington in fall 2016, and had the opportunity to work as a graduate research/teaching assistant under the supervision of Dr. Sahadat Hossain. The author's research interests include sustainable waste management systems, bioreactor landfills, landfill final cover system design, biocells, constitutive modeling of soil, numerical modeling, deep foundations, slope stability analysis, non-destructive testing, and geophysical investigations.